

VISUAL TRANSDUCTION IN CONES OF THE MONKEY *MACACA FASCICULARIS*

By J. L. SCHNAPF*, THE LATE B. J. NUNN, M. MEISTER AND D. A. BAYLOR
*From the Department of Neurobiology, Stanford Medical School, Stanford, CA 94305, USA and *Departments of Ophthalmology and Physiology, University of California, San Francisco, CA 94143, USA*

(Received 16 October 1989)

SUMMARY

1. Visual transduction in macaque cones was studied by measuring the membrane current of single outer segments projecting from small pieces of retina.

2. The response to a brief flash of light was diphasic and resembled the output of a bandpass filter with a peak frequency near 5 Hz. After the initial reduction in dark current there was a rebound increase which resulted from an increase in the number of open light-sensitive channels. The response to a step of light consisted of a prominent initial peak followed by a steady phase of smaller amplitude.

3. Responses to dim light were linear and time-invariant, suggesting that responses to single photons were linearly additive. From the flash sensitivity and the effective collecting area the peak amplitude of the single photon response was estimated as about 30 fA.

4. With flashes of increasing strength the photocurrent amplitude usually saturated along a curve that was gentler than an exponential but steeper than a Michaelis relation. The response reached the half-saturating amplitude at roughly 650 photoisomerizations.

5. The response–intensity relation was flatter in the steady state than shortly after a light step was turned on, indicating that bright light desensitized the transduction with a delay. This desensitization was not due to a reduction in pigment content. In the steady state, a background of intensity I lowered the sensitivity to a weak incremental test flash by a factor $1/(1+I/I_0)$, where I_0 was about 2.6×10^4 photoisomerizations s^{-1} , or about 3.3 log trolands for the red- and green-sensitive cones.

6. Bleaching exposures produced permanent reductions in flash sensitivity but had little effect on the kinetics or saturating amplitude of subsequent flash responses. The sensitivity reductions were consistent with the expected reductions in visual pigment content and gave photosensitivities of about $8 \times 10^{-9} \mu m^2$ (free solution value) for the red- and green-sensitive pigments. During a steady bleaching exposure the final exponential decline of the photocurrent had a rate constant given by the product of the light intensity and the photosensitivity.

7. In some cells it was possible to measure a light-induced increase in current noise. The power spectrum of the noise resembled the spectrum of the dim flash

response and the magnitude of the noise was consistent with a single photon response roughly 20 fA in size.

8. The membrane current recorded in darkness was noisy, with a variance near 0.12 pA^2 in the band 0–20 Hz. The power spectrum of the dark noise resembled the spectrum of the dim flash response. Noise with the observed magnitude and spectral composition would be generated by photoisomerizations occurring at a rate of about 2400 s^{-1} .

INTRODUCTION

Until recently, physiological studies on primate cones have been limited by the small size and fragility of the cells. Some information has been obtained by recording summated light responses from cell populations (e.g. Boynton & Whitten, 1970; Valeton & van Norren, 1983), but a clearer picture of the functional properties of the cones requires analysis at the single-cell level. For example it is difficult to determine the kinetics and intensity dependence of the light responses from massed recordings because the measured signals often consist of multiple components, some not of cone origin. Furthermore, massed recordings give no information about response fluctuations, nor about cell noise in the dark.

Suction electrodes allow stable recordings to be made from a single primate photoreceptor for an hour or more. Previously we used this method to study transduction by macaque rods (Baylor, Nunn & Schnapf, 1984), and to measure the spectral sensitivity of macaque and human cones (Baylor, Nunn & Schnapf, 1987; Schnapf, Kraft & Baylor, 1987). Here we examine the kinetics and sensitivity of the cone photocurrents, the effects of background light and pigment bleaching, and the magnitude and frequency composition of the membrane current noise.

METHODS

Preparation

Retinas were obtained from male monkeys, *Macaca fascicularis*, which were donors in heart–lung transplant experiments in the Department of Cardiovascular Surgery, Stanford University School of Medicine. Enucleation was performed under full anaesthesia immediately prior to the transplantation. Induction was by ketamine (10 mg/kg, i.m.) followed by Nembutal (total 10–35 mg/kg, i.v.); the dose of Nembutal was increased until deep stage III surgical anaesthesia was obtained, evidenced by absence of nociceptive reflexes and slow, deep respirations at a regular rate. The eye was dark adapted by placing an opaque contact lens over the anaesthetized animal's cornea 30 min before enucleation.

The retina was isolated, stored, and chopped into small pieces using procedures described previously (Baylor *et al.* 1984, 1987). During preparation of the tissue, exposure to visible light was minimized by using dim red light or infra-red light and infra-red/visible image converters. The preparation was viewed with an inverted microscope equipped with an infra-red sensitive video camera; the video monitor was located outside the light-tight box enclosing the preparation. Preparations were made from both central and peripheral portions of the retina. Central retina was obtained by visualizing the fovea and excising a 1–2 mm square piece of retina containing it (Baylor *et al.* 1987). Some outer segments were wrinkled, bent, or rounded up, but there was no obvious correlation between an outer segment's appearance and its physiological behaviour.

Solutions

Retinas were isolated in oxygenated HEPES Locke solution that contained (mM): Na^+ , 140; K^+ , 3.6; Ca^{2+} , 1.2; Mg^{2+} , 2.4; Cl^- , 151; HEPES buffer, 3 (pH 7.4); D-glucose, 10; EDTA, 0.02. Pieces of isolated retina were stored in light-tight containers at 5 °C in L-15 tissue culture medium (GIBCO) containing 0.02 mM-EDTA and 0.01 % gentamicin. During recordings the experimental chamber

was perfused with bicarbonate-buffered Locke solution equilibrated with 95% O₂-5% CO₂ and kept at 37 °C. This solution was identical to HEPES Locke except that 20 mM-NaHCO₃ replaced an equal concentration of NaCl.

Membrane current recording

Membrane current was recorded from cone outer segments protruding from small pieces of retina. A single outer segment was drawn into a fire-polished, silanized glass pipette connected to a current-to-voltage converter. The output of the current-to-voltage converter was stored on an FM tape-recorder at a bandwidth of 0-330 Hz. A feedback circuit held the voltage in the recording chamber at ground potential, reducing electrical noise caused by perfusion of the chamber.

When membrane current recordings were later digitized for computer analysis, they were replayed through an 8-pole Bessel or 6-pole Butterworth filter with a cut-off frequency chosen to prevent aliasing. Where indicated, some records were further processed by a digital low-pass filter (Colquhoun & Sigworth, 1983).

Light stimuli and cell identification

Cones were stimulated with unpolarized light from a dual-beam optical stimulator (Baylor & Hodgkin, 1973). The beam passed through the outer segment approximately perpendicular to its long axis. Usually the light was applied as a spot 300 μm in diameter. The size of the stimulus did not influence the response except by lowering the intensity at the cell when the spot was very small. Local illumination of the outer segment gave responses similar to those observed with diffuse illumination, suggesting that the measured responses were not affected by interactions between cells. The stimulating light was made monochromatic by interference filters with 10 nm nominal half-bandwidths. The intensity was controlled with calibrated neutral density filters. The source intensity was calibrated at the end of each experimental day. For simplicity, light intensities are expressed as equivalent intensities at the cell's optimum wavelength: 430 nm for the blue-sensitive cones, 530 nm for green and 560 nm for red. Intensity conversions were made using the tabulated values for average spectral sensitivity in Baylor *et al.* (1987). Usually the stimulus was a flash with a width at half-height of 10.7 ms and rise and fall times of 1 ms. Because the flash width is short compared to the cone's response to a dim flash (time to peak ~ 50 ms) this stimulus approximates an impulse.

Each cone's spectral type was determined from its sensitivity to flashes at 440, 500 and 660 nm (Baylor *et al.* 1987). Rods were distinguished by their different morphology, different relative sensitivities at the three test wavelengths, slower response kinetics, and larger absolute sensitivities (Baylor *et al.* 1984, 1987).

Collecting area of outer segment

The rate at which a light of known intensity will photoisomerize a cone's pigment can be estimated if the effective collecting area of the outer segment is known (Baylor & Hodgkin, 1973). For transversely incident unpolarized light at the optimal wavelength, a fixed collecting area A_c of 0.37 μm² is adopted on the following basis. The volume of nine outer segments, calculated from dimensions in photographs from the video monitor, was 30 ± 10 μm³ (mean ± s.d.); the inner segments of the same cells ranged in diameter from 2.8 to 11.5 μm, indicating that the retinal locations of the cones varied widely along the central-to-peripheral dimension. There was no indication that outer segment volume varied systematically with retinal location. Using a volume of 30 μm³ in eqn (14) of Baylor, Lamb & Yau (1979), assuming a quantum efficiency for photoisomerization of 0.67 (Dartnall, 1972), and taking the peak axial pigment density as 0.016 μm⁻¹ (Harosi, 1975) gives $A_c = 0.37 \mu\text{m}^2$.

Expression of light intensity in trolands

To facilitate comparison of results we have expressed some light intensities in trolands, a unit of retinal illuminance commonly used in psychophysical experiments on cone vision. One troland is equivalent to an intensity I_{ax} , incident on the retinal surface in a direction parallel to the long axis of the outer segments, given by

$$I_{ax} = 2.649 \times 10^{-2} \text{ photons } \mu\text{m}^{-2} \text{ s}^{-1} \text{ nm}^{-1} \lambda t(\lambda) / V(\lambda), \quad (1)$$

where λ is the wavelength in nm, $t(\lambda)$ is the effective preretinal transmittance of the eye and $V(\lambda)$ is the photopic luminosity at λ (Wyszecki & Stiles, 1982, p. 105). The equivalence at 560 nm, for

example, is obtained as follows. Taking $V(560)$ as 0.995 (Wyszecki & Stiles, 1982, p. 256) and $t(560)$ as 0.87 (Wyszecki & Stiles, 1982, p. 721; Baylor *et al.* 1987) one obtains $I_{ax} = 13.0$ photons $\mu\text{m}^{-2} \text{s}^{-1}$. Now transversely incident unpolarized light, as used here, is absorbed less strongly than axially incident light. The transverse intensity I_{tr} equivalent in its effect to axial intensity I_{ax} is

$$I_{tr} = I_{ax} F A_{ax} / A_c, \quad (2)$$

where A_{ax} and A_c denote the collecting areas of the outer segment for axial and transverse illumination and F is the factor by which the inner segment concentrates the light incident on the outer segment. Taking the outer segment as a cylinder, the ratio of the collecting areas is approximately

$$A_{ax} / A_c = (1 - 10^{-D}) / 0.5D \ln(10), \quad (3)$$

where D is the optical density of the outer segment for axial light. Taking D for the red-sensitive and green-sensitive cones as 0.27 (Baylor *et al.* 1987), the ratio $A_{ax} / A_c = 1.49$. From the ratio of the relative cross-sectional areas of the inner and outer segments in the fovea, the value for F is taken as 2. The exact magnitude of this focusing effect is uncertain.

One troland, therefore, corresponds to $1.49 \times 13.0 \times 2 = 38.7$ photons $\mu\text{m}^{-2} \text{s}^{-1}$ in our experiments. Since at 560 nm D for the blue-sensitive cones is much smaller (Baylor *et al.* 1987), one troland at this wavelength is equivalent to 51.8 photons $\mu\text{m}^{-2} \text{s}^{-1}$ for the blue-sensitive cones.

These equivalences do not depend strongly on the shape or pigment density of the outer segment. They do depend on light concentration by the inner segment, however, an effect whose magnitude needs to be determined more accurately.

RESULTS

Responses to flashes of increasing strength

Flash response families from a blue-, green- and red-sensitive cone are shown in Fig. 1. All three families had diphasic waveforms. The reduction of the inward current was followed by a rebound increase, or 'undershoot.' In some cells there was a small final oscillation in which the inward current again decreased. Unlike responses of turtle cones (Baylor, Hodgkin & Lamb, 1974), there was little if any shortening in the time to the peak of the initial phase as the flash strength was raised.

The relation between the amplitude of the positive phase and the flash strength is illustrated in Fig. 2A, which presents results from five cells with large responses, including those of Fig. 1. The ordinate is the peak response amplitude r relative to its maximal value r_{max} , while the log abscissa is the flash strength i multiplied by a constant k characteristic of each cell. This constant, termed the cell's normalized flash sensitivity, is defined as

$$k = r / i r_{max}, \quad (4)$$

for small responses, i.e. $r \ll r_{max}$. For the five cells, r_{max} varied between 10 and 30 pA, while values for k varied between 2.87×10^{-4} and 1.71×10^{-3} photons $^{-1} \mu\text{m}^2$. In twenty-five cells the average value of the photon density, $i_{\frac{1}{2}}$, required to elicit a half-maximal response was 1.75×10^3 photons μm^{-2} , or 648 photoisomerizations; individual values are given in Table 1.

The continuous curves in Fig. 2A show attempts to fit the experimental results by three equations. Curve I was drawn according to the exponential saturation characteristic:

$$r / r_{max} = 1 - \exp(-ki). \quad (5)$$

As reported previously (Baylor *et al.* 1987), this function gives a fair description,

although it saturates more sharply than the responses of some cells. Curve II was drawn according to the Michaelis relation:

$$r/r_{\max} = i/(i + 1/k). \quad (6)$$

This curve saturates too gently. Curve III, which fits best, is the average of relations (5) and (6), with relation (5) weighted three times more heavily than relation (6).

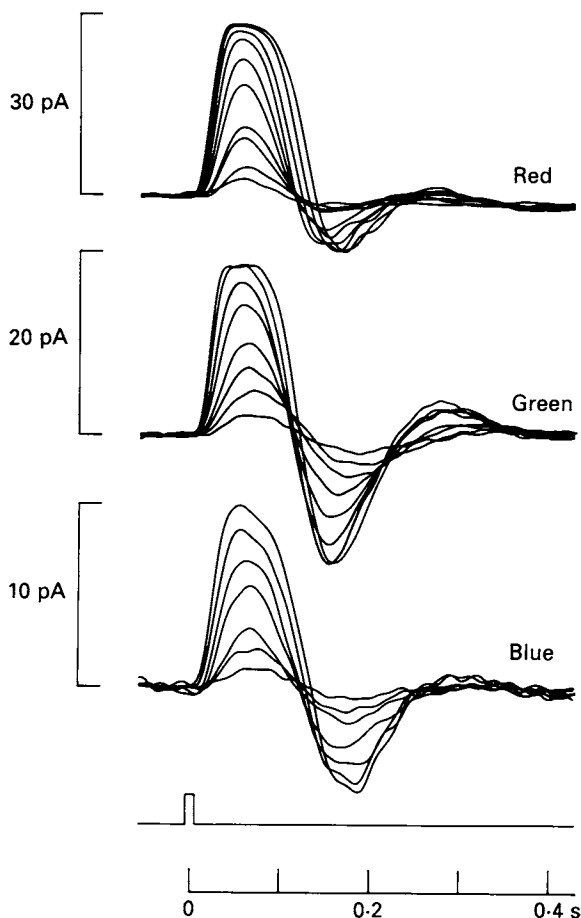


Fig. 1. Response families from three cells. Superimposed responses to flashes of increasing strength, with the change in membrane current from the dark level plotted as a function of time from the centre of the 10.7 ms flash. Flash strengths at the optimum wavelengths varied by nominal factors of 2 between 3.72×10^2 and 1.64×10^4 photons μm^{-2} for the blue-sensitive cone, 7.80×10^1 and 5.35×10^3 photons μm^{-2} for the green-sensitive cone, and 1.78×10^2 and 3.86×10^4 photons μm^{-2} for the red-sensitive cone. Each trace was averaged from two to fourteen sweeps and digitally filtered, DC–25 Hz. Cells 12, 14 and 26 in Table 1.

Although curve III fits all the results in Fig. 2A reasonably well, other cells had slightly steeper or gentler saturation characteristics closer to eqn (5) or (6) respectively (Table 1).

Figure 2B plots the relative undershoot amplitude as a function of flash strength.

TABLE 1. Response properties of cells with large responses

Cell	Type	$r_{\max+}$ (pA)	$r_{\max-}$ (pA)	$i_{\frac{1}{2}}$	Fit	TTP (ms)	τ_1 (ms)	S/P	a (fA)
1	R	14	7	1015	0.38	80	30	0.60	31
2	R	24	10	1180	0.75	50	25	0.48	38
3	R	19	6	321	0.50	72	—	—	112
4	R	22	11	472	0.75	85	55	0.50	97
5	R	16	10	3656	1.0	48	11	0.27	8
6	R	14	8	6856	0.75	38	—	—	4
7	R	28	13	406	0.75	75	28	0.44	119, 32
8	R	16	8	1912	0.13	42	17	0.42	22
9	R	20	10	1463	1.0	40	18	0.50	26, 15
10	R*	12	2	2101	0.50	38	44	0.70	13
11	R*	19	8	1487	0.75	40	17	0.50	27, 16
12	R*	30	9	1227	0.75	50	35	0.65	51
Red mean		20	8	1841	0.67	55	28	0.51	46
s.d.		6	3	1822	0.25	18	14	0.12	41
13	G	13	11	1018	1.0	58	8	0.17	24
14	G	19	16	520	0.75	58	12	0.33	76
15	G	18	15	1460	1.0	38	33	0.48	23
16	G	15	11	2478	0.75	40	10	0.20	12
17	G	14	5	2567	0.25	50	35	0.59	14
18	G	20	9	—	—	65	10	0.34	30
19	G*	12	8	1150	0.88	75	15	0.25	21
20	G*	12	9	2213	1.0	55	23	0.31	10, 17
21	G*	13	10	1170	1.0	40	24	0.53	21, 8
22	G*	14	9	1611	0.38	48	29	0.63	21
23	G*	26	12	2204	0.25	30	15	0.38	29
Green mean		16	10	1639	0.73	51	19	0.38	26
s.d.		4	3	695	0.32	13	10	0.16	18
24	B*	9	2	1851	0.75	60	46	0.85	10
25	B*	5	3	929	1.0	62	22	0.32	10
26	B*	11	6	2415	0.63	62	—	—	10
Blue mean		8	4	1732	0.79	61	34	0.58	10
s.d.		3	2	750	0.19	1	17	0.37	0
Grand mean		17	9	1747	0.71	54	24	0.45	33

Asterisks indicate cells within 1 mm of the fovea; $r_{\max+}$ the maximum amplitude of the positive-going portion of the flash response; $r_{\max-}$ the maximum size of the negative-going portion; $i_{\frac{1}{2}}$ is flash strength (in photons μm^{-2} at λ_{\max}) needed to evoke a response of $0.5 r_{\max+}$; fit is the relative weighting of eqns (5) and (6) needed to give the best fit to the flash strength *vs.* response amplitude relation, where 1.0 indicates exclusively eqn (5) and 0 indicates exclusively eqn (6); TTP is time to peak of linear flash response; τ_1 is integration time; S/P is the ratio of the amplitudes in the steady state and at the peak of the response to a dim step of light; a is the peak amplitude of the single photon response as estimated from dim flash sensitivity, and from noise in dim light (second entry).

The curve is the same as curve III in Fig. 2*A*. Initially the undershoot increased in proportion to the positive phase, but with very bright flashes the undershoot became progressively smaller.

Linearity of responses to dim light

The results in Fig. 2 suggest that the peak amplitude of both phases of the flash response scaled linearly with flash strength when the amplitude of the response was

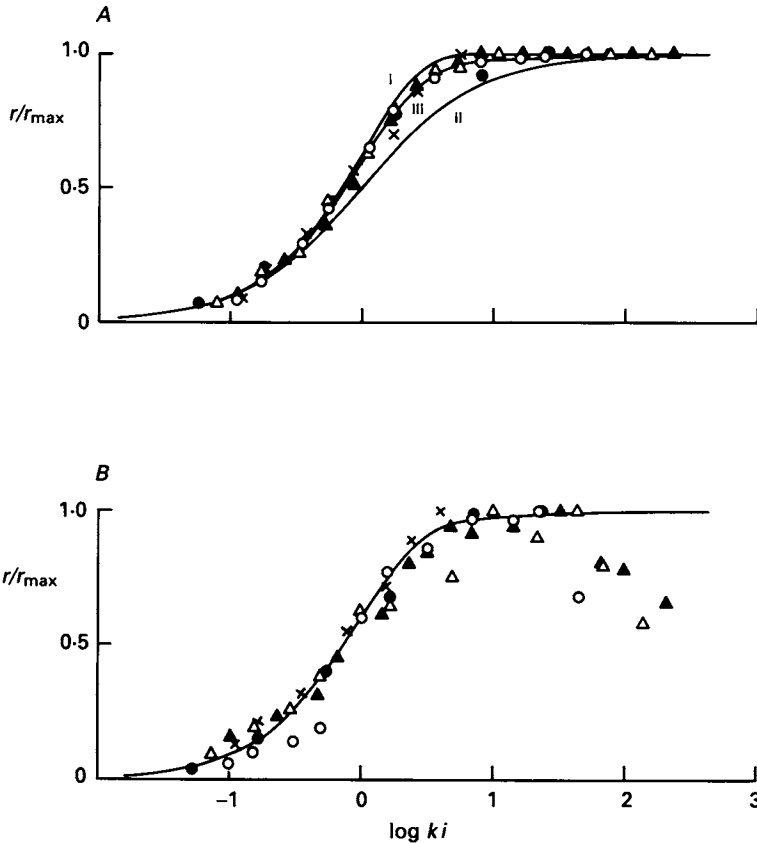


Fig. 2. *A*, relation between amplitude of positive (initial) phase of flash response and flash strength. Peak photocurrent amplitude r , normalized by the maximal amplitude r_{\max} , plotted as a function of normalized flash strength ki . Collected results from five cells, each plotted by a different symbol (Δ , \circ , red-sensitive cones; \blacktriangle , \bullet , green; \times , blue). Continuous curves described in text. *B*, relation between undershoot amplitude and flash strength, on same abscissa as in *A*; ordinate normalized to the maximal amplitude of the undershoot. Curve same as III in *A*. Cell parameters given in Table 1; cell numbers and symbols are: 7, Δ ; 12, \circ ; 14, \blacktriangle ; 23, \bullet ; 26, \times .

small. A linear dependence in dim light has been observed in a variety of vertebrate photoreceptors, both rods and cones, and is expected when the conductance change resulting from absorption of a photon is spatially restricted.

The experiments of Fig. 3 were performed to test the linearity of the response more

stringently. Figure 3*A* demonstrates that the entire waveform of the dim flash response scaled linearly with flash strength. The bold traces are averaged responses from a red-sensitive cone to flashes at strengths varying over a 7-fold range. Near the experimental responses are thin lines showing the expectations if responses with a

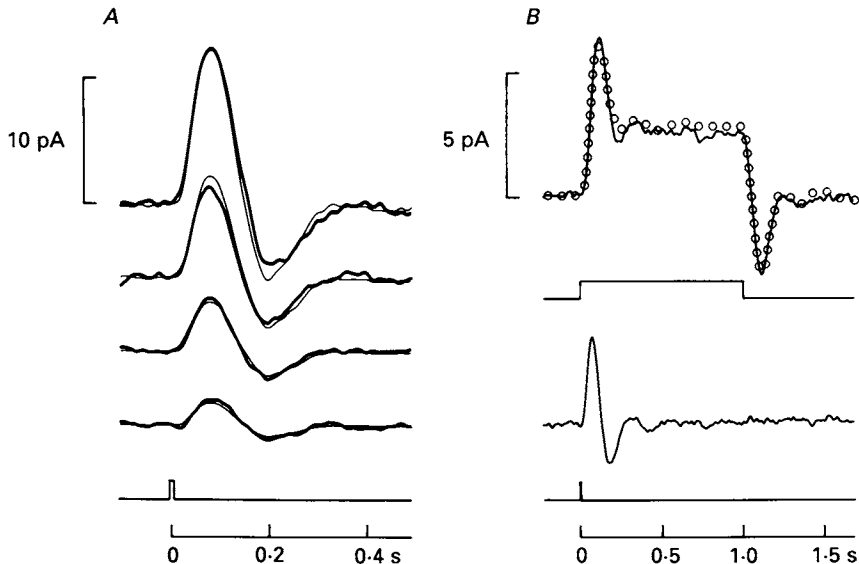


Fig. 3. Linearity and time-invariance of light responses from a red-sensitive cone. Change in membrane current plotted as a function of time; stimulus monitor shown below current traces. *A*, linearity of dim flash response. Bold traces are averaged responses to brief flashes at strengths varied by nominal factors of two. Thin curves have the form of the sum of all the responses. Individual thin curves were scaled by the flash strength in that trial divided by the total strength over all trials. Response averages calculated from five to sixteen sweeps. Flash strengths, from below upwards were (photons μm^{-2}): 41.6, 91.1, 187, 283. *B*, time-invariance of transduction. Recordings of average responses to a brief flash and a long pulse of light, which were alternated during a run of forty-six presentations. Open circles show the pulse response predicted by linear superposition of the flash responses. Pulse intensity 2350 photons $\mu\text{m}^{-2}\text{s}^{-1}$, flash strength 91.1 photons μm^{-2} . Records in *A* and *B* digitally filtered DC–20 Hz. Maximum response amplitude 28 pA. Cell 7 in Table 1.

fixed shape simply scaled in proportion to flash strength. The thin lines were calculated by the procedure of Baylor & Hodgkin (1973): responses to flashes at all four strengths were summed and scaled by the ratio of the flash strength in each trial to the average strength in all trials. The interpretation of Fig. 3*A* is that single photon responses with an average shape like that of the thin curves summed linearly to produce the macroscopic response. No cells exhibited significant deviations from linearity when the response amplitude was less than about $\frac{1}{3}$ maximal. From the measured flash sensitivities and an assumed collecting area of $0.37 \mu\text{m}^2$, the average photon response amplitude from twenty-six cells was 33 fA.

Figure 3*B* demonstrates that the transduction was time-invariant in dim light. A brief flash and a long pulse were given repeatedly and the average responses plotted. If single photon effects add independently during a long pulse, then the response to

the pulse should have the form of the time integral of the flash response, with a vertical scaling determined by the relative flash and step intensities and the flash duration. The prediction of this notion, shown by the open circles, agreed well with the experimental response. Experiments like that of Fig. 3B were performed on a

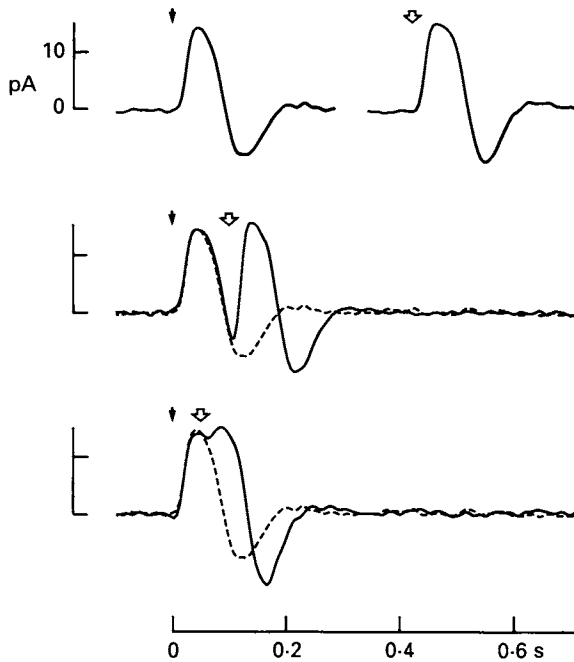


Fig. 4. Suppression of a red-sensitive cone's undershoot current by a second bright flash. Upper trace, responses to conditioning and test flash alone. Lower traces, responses to both flashes. Dashed lines plot the conditioning response on its own. Flash timing indicated by arrows. Each trace the average of four to six sweeps. Flash strengths (in photons μm^{-2}) were: 6160 (first) and 13000 (second). Bandwidth 0–30 Hz.

total of three cells, and in all cases the observed and calculated pulse responses were in good agreement.

Origin of undershoot

The undershoots reported here (e.g. Figs 1 and 3) are more prominent than those reported previously in other vertebrate photoreceptors (e.g. Baylor & Hodgkin, 1973; Schnapf & McBurney, 1980; Kraft, 1988) except human cones (Schnapf *et al.* 1987). The experiment of Fig. 4 demonstrates that the undershoot consists of an increase in the current through the light-sensitive channels. Responses to two flashes of saturating strength were presented alone (uppermost traces) or in succession. The second flash completely shut off the undershoot current in the first response (middle trace), or delayed the appearance of the undershoot (lowest trace). The same result was obtained on two other cells.

The increased current during the undershoot could result from membrane

hyperpolarization or an increase in the number of open light-sensitive channels. The experiment illustrated in Fig. 5 suggests the latter possibility. After this cell had been studied for some time it began to give large action potentials; similar spikes were occasionally seen in other cells after a long period of recording or after the inner

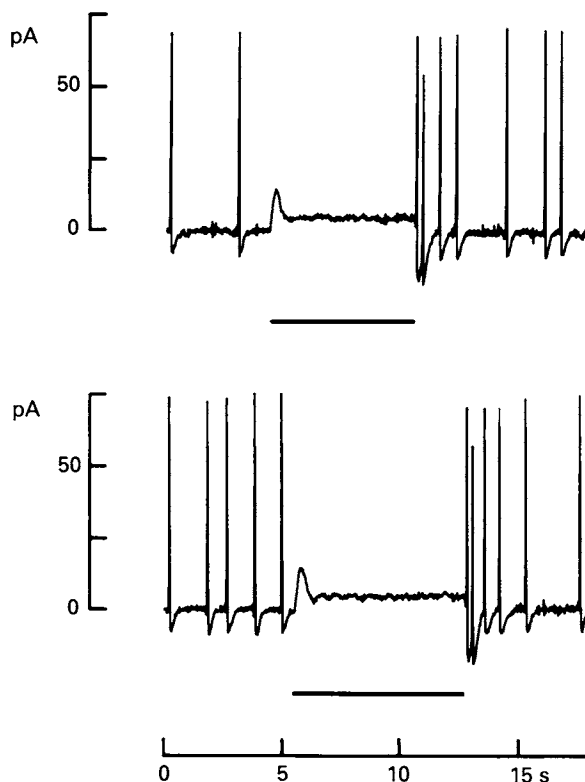


Fig. 5. Change in spike frequency, an indicator of membrane potential, during a red-sensitive cone's response to a light pulse. Outer segment current as a function of time, with pulse timing shown by the bars under the records. The action potentials, which presumably resulted from damage to the cell, occurred at low frequency in darkness, were suppressed by the pulse and accelerated when the light went off. Maximum photocurrent amplitude 15 pA, bandwidth 0–30 Hz. Pulse intensity 2.58×10^4 photons $\mu\text{m}^{-2} \text{s}^{-1}$.

segment was squeezed by a narrow suction electrode. The positive initial polarity suggests that the spikes arose in the cone inner segment; it seems likely that they resulted from regenerative activity of voltage-sensitive calcium channels (Piccolino & Gerschenfeld, 1978). We assume that the frequency of occurrence of spikes increases with depolarization and thus provides a measure of the cone's membrane potential. Consistent with this notion, spikes were absent during the response to light, when the cone presumably hyperpolarized. When the light was turned off, firing accelerated, indicating that the membrane depolarized during the undershoot. A depolarization is expected if the number of open light-sensitive channels increased. These results suggest that the undershoot is generated by a rebound increase in the light-sensitive conductance rather than by activation of synaptic or voltage-

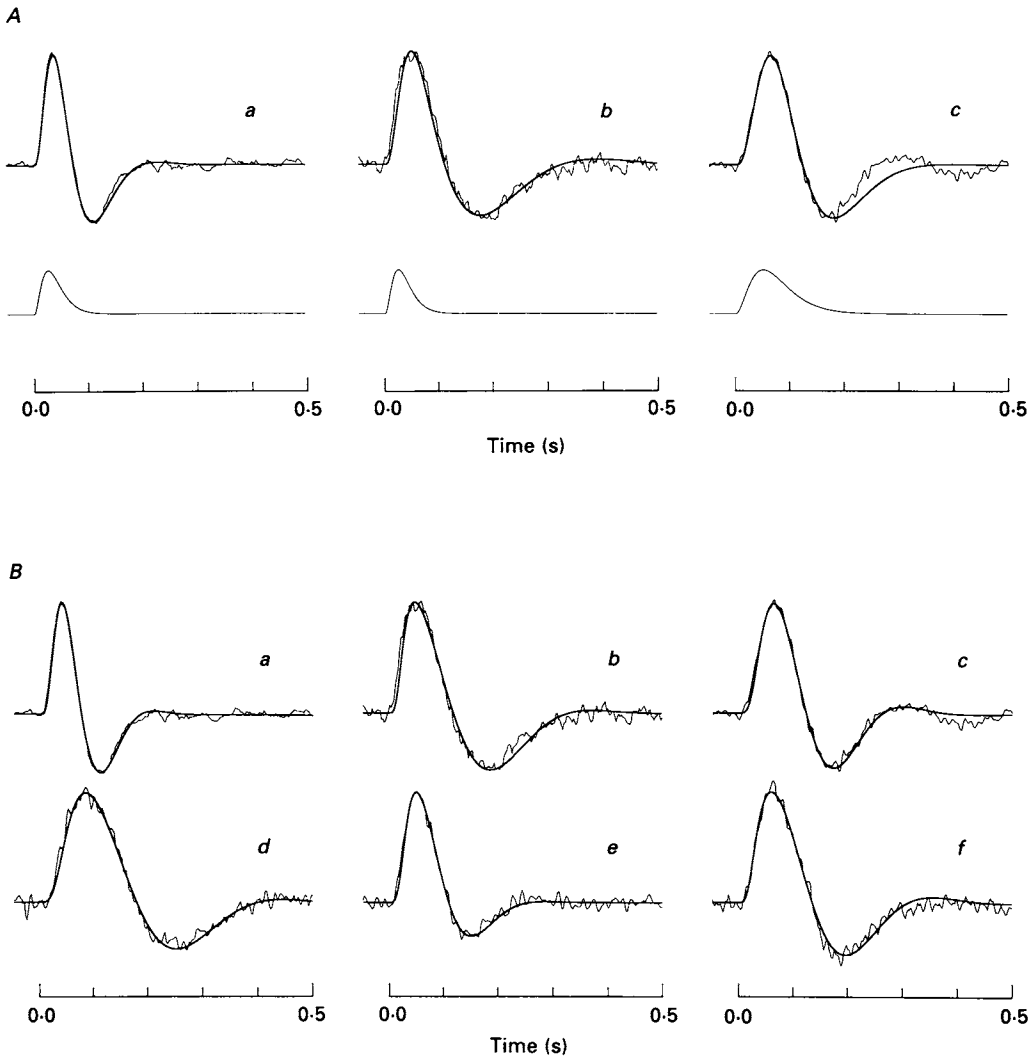


Fig. 6. *A*, linear flash responses from three cones (thin lines) fitted by eqn (19) of the negative feedback model presented in the Appendix (bold lines). Experimental traces are average dim flash responses, normalized to the same peak amplitude. Cells *a* and *c* were red-sensitive cones and *b* was green-sensitive. The origin on the time axis of the experimental responses is taken 5 ms after the centre of the 11 ms flash to allow for the lag introduced by the 0–100 Hz Bessel low-pass filter. For calculating the model's responses, the phosphodiesterase activity was assumed to follow eqn (18); this activity, normalized to its peak value, is plotted at the bottom of each panel. *B*, linear flash responses from six cones (thin lines) fitted by the empirical expression of eqn (7) (bold lines). Cells *a*, *b* and *c* are those of *A*; *d* was red-sensitive, *e* green, and *f* blue. Parameters used in eqns (7), (18) and (19) are given in Table 2. For some cells, other response parameters are given in Table 1; cell numbers in Table 1 are: 5, *a*; 7, *c*; 4, *d*; 17, *e* and 25, *f*.

dependent conductances. Voltage-clamp experiments could clinch this interpretation.

Kinetics of linear responses to dim light

Is the time course of the linear flash response consistent with known biochemical processes in the outer segment? These processes form the negative feedback loop diagrammed in Fig. 15 and analysed quantitatively in the Appendix. It is our purpose here to test whether this model, which is based on the results of other groups (see reviews by Hodgkin, 1988; Stryer, 1988), can explain the kinetics of the primate cone responses. In this model, a decrease in 3'-5'-cyclic guanosine monophosphate (cyclic GMP) concentration closes cation channels in the plasma membrane, leading to a decreased influx of Ca^{2+} . Persistent activity of the $\text{Na}^+/\text{Ca}^{2+}\text{-K}^+$ exchanger (Cervetto, Lagnado, Perry, Robinson & McNaughton, 1989) causes the intracellular Ca^{2+} level to drop. The drop in Ca^{2+} activates the guanylate cyclase that synthesizes cyclic GMP (Koch & Stryer, 1988). The cyclic GMP level rises, opening more channels and increasing the influx of Ca^{2+} . This system stabilizes the levels of cyclic GMP and Ca^{2+} in the dark and assists recovery after a light-induced pulse of phosphodiesterase (PDE) activity. The treatment in the Appendix shows that after a brief PDE pulse the current recovers with a damped oscillation. The damping time and frequency of the oscillation depend on the time constants for turnover of cyclic GMP (τ_{cG}) and Ca^{2+} (τ_{Ca}) as well as the strength of the effects of cyclic GMP and Ca^{2+} on the channel and the guanylate cyclase respectively.

Figure 6A compares the time course of the linear flash responses of three cones (thin traces) with the prediction of eqn (19) of the Appendix (heavy traces). The theoretical curves were computed assuming that the flash-induced PDE pulse took the form of the impulse response of three buffered low-pass filters, as the measured flash response rose with a slope of 3 when plotted on double logarithmic co-ordinates (Baylor *et al.* 1974). For simplicity, the time constants of these filters (τ_{PDE}) were taken to be equal. Fits of similar quality to those in Fig. 6A were obtained for six other cells. The recovery phase of the responses in some cells deviated slightly from the theoretical function (e.g. Fig. 6A, cell *c*). For the nine cells, the best-fitting values of the time constants were (mean \pm s.d.): 29 ± 11 ms (τ_{cG}), 870 ± 330 ms (τ_{Ca}), and 19 ± 6 ms (τ_{PDE}).

The fits worsened if τ_{PDE} or τ_{cG} were changed by 20% or more, or if τ_{Ca} was changed by more than 30%. For given values of the time constants, acceptable fits were still obtained when the gain factor bc was changed from the assumed value of -12 to -9 . At a gain of -6 the fits worsened appreciably unless τ_{Ca} was decreased. For gains more positive than -4 no acceptable fits could be obtained.

While the exact form of the PDE pulse is uncertain, acceptable fits required the duration of the pulse to be briefer than the impulse response of the loop and the duration of the photocurrent. With a longer PDE pulse, the calculated photocurrent was no longer oscillatory.

The mean Ca^{2+} turnover time is slightly longer than that determined experimentally for amphibian rods (e.g. Hodgkin, 1988), while the cyclic GMP turnover time is an order of magnitude shorter. Our analysis leaves some uncertainty, however, about the relative values of these two turnover times. This is because both

the frequency of oscillation and the damping time of the loop's impulse response are invariant under exchange of the values of τ_{Ca} and τ_{cG} (see expressions for p and q in eqn (15)). Only the phase of the oscillation reveals the ratio of τ_{Ca} and τ_{cG} , but the phase inferred from the flash response depends on the assumed time course of the light-induced PDE activity, about which we have no direct information. For the

TABLE 2. Parameters used in eqns (7), (18) and (19) for fitting the theoretical functions to the experimental traces in Fig. 6

Cell	τ_{PDE} (s)	τ_{cG} (s)	τ_{Ca} (s)	τ_r (s)	τ_d (s)	τ_p (s)	ϕ (deg)
a	0.013	0.020	0.45	0.025	0.11	0.22	-31
b	0.012	0.050	0.80	0.025	0.20	0.42	-10
c	0.025	0.025	0.73	0.035	0.18	0.28	-65
d				0.045	0.25	0.43	-58
e				0.030	0.13	0.30	-39
f				0.030	0.21	0.35	-47

class of PDE waveforms assumed here the best fits were always obtained with τ_{Ca} larger than τ_{cG} .

We emphasize that the estimated values of the parameters depend on the simplifying assumptions on which the model is based. Non-linearities have not been considered here, and if significant would alter the estimates. Diffusional delays have not been taken into account because their magnitudes are not known. Likewise, the action of calcium on the cyclase, which involves a soluble co-factor (Koch & Stryer, 1988), might also introduce delay. None the less, the correspondence between the simplified theoretical treatment and the experimental curves of Fig. 6A seems reasonable, as do the estimated values for the turnover times. The oscillatory flash response therefore seems consistent with a negative feedback loop involving Ca^{2+} and cyclic GMP. Direct determination of the parameters of the loop remains an important goal for future work.

A simple empirical expression that also gave a good description of the linear flash response $j(t)$ is:

$$j(t) = j_0 \frac{(t/\tau_r)^3}{1 + (t/\tau_r)^3} \exp[-(t/\tau_d)^2] \cos(2\pi t/\tau_p + \phi). \quad (7)$$

In this expression, which describes a damped oscillation with an S-shaped onset, τ_r determines the rising phase, τ_d the damping time, τ_p the period, ϕ the phase, and j_0 is a scaling constant. Figure 6B shows linear flash responses from six cells fitted with this expression; the parameters used to make the fits are given in Table 2.

There was little evidence that the sensitivity or time scale of the linear responses varied systematically with cone type (red-, green- or blue-sensitive) or retinal location. The time to the peak of the dim flash response was 55 ± 18 ms (mean \pm s.d.) for the twelve red-sensitive cones in Table 1 and 51 ± 13 ms for the eleven green-sensitive cones. For fifteen peripheral red- and green-sensitive cones the time to peak was 56 ± 16 ms, while for eight red- and green-sensitive cones within 1 mm of the fovea the figure was 47 ± 14 ms. Only a few blue-sensitive cones were studied, but

their kinetics and sensitivity were roughly comparable to those of the red- and green-sensitive cones. There was a suggestion that the step response of the green-sensitive cones was more transient than that of the red. The ratio of the final and peak step response amplitudes was 0.51 ± 0.12 (mean \pm s.d.) for the ten red-sensitive cones of Table 1, while for the eleven green-sensitive cones it was 0.38 ± 0.16 . The integration time, τ_i , obtained from the time integral of the linear flash response normalized to a peak height of one (Baylor & Hodgkin, 1973), was 28 ± 14 and 19 ± 9.8 (mean \pm s.d.) for the red- and green-sensitive cones respectively.

The time integral of the positive lobe of the normalized flash response was about 50 ms. For a given intensity, a pulse of this duration will elicit a response with the largest peak amplitude. This duration corresponds roughly to the integration time of the photopic system determined psychophysically (Hood & Finkelstein, 1986).

Desensitization by non-bleaching backgrounds

This section shows that bright steady light reduced the amplitude of photon responses by two mechanisms that did not depend upon reduction in the cone's pigment concentration. This latter effect ('bleaching') does become important in very bright light and is treated below. The first mechanism is an instantaneous saturation: elementary excitations, with shapes like that of the single photon effect, add linearly in dim light but must compete to close light-sensitive channels in bright light. If most of the channels are already closed, additional photons can have little effect (Lamb, McNaughton & Yau, 1981). This saturation has been extensively described; it produces the characteristic form of the curves in Fig. 2. The second mechanism scales down the elementary excitation at a point in transduction that precedes the instantaneous saturation. In monkey cones, activation of this mechanism is graded with the intensity of the steady light and requires times of the order of a second to become appreciable.

Figure 7 illustrates these points. Figure 7A shows a cone's responses to light steps of increasing intensity, while the plots in Fig. 7B give the dependence of response amplitude on step intensity at several fixed times after step onset. The relations at 64 and 114 ms were fitted satisfactorily by the continuous curves, which have the form of the saturation characteristic measured with brief flashes (curve III of Fig. 2). The curves lie at horizontal positions predicted by the time integral of the cell's dim flash response (see Fig. 3B). The good match between the measured responses and theoretical curves for times up to about 0.1 s after light onset indicates that elementary excitations summed in a linear and time-invariant manner even in the brightest light, then were subject to the instantaneous saturation. At 1 and 2 s after onset of the step, the observed response-intensity relations were flatter, suggesting a progressive reduction in sensitivity at high intensities (Baylor & Hodgkin, 1974). The slow droop in the responses to the three brightest steps in Fig. 7A is attributed to the onset of this gain reduction. The droop was not due to a drop in the cone's ability to absorb, as the total reduction in visual pigment concentration was calculated to be less than 10% in the entire experiment (see p. 699).

The effect of steady background light on incremental sensitivity was probed by presenting test flashes on backgrounds. The flashes were kept dim so that they did not appreciably change the state of the transduction mechanism and so that the

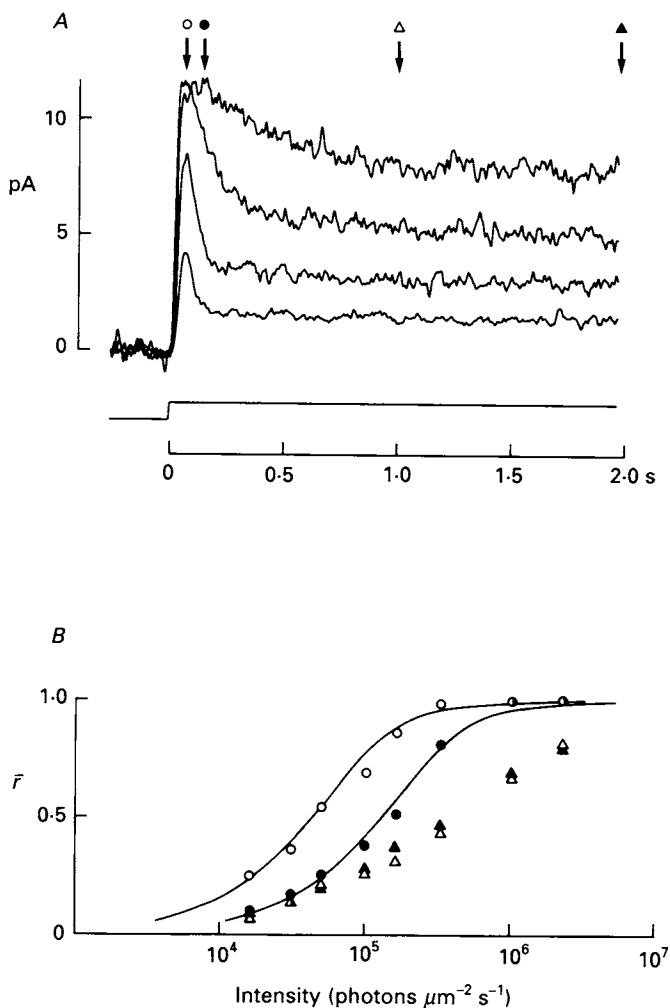


Fig. 7. Dependence of a green-sensitive cone's step response amplitude on step intensity. *A*, step responses. Change in membrane current plotted as a function of time after step onset, with stimulus monitor below. Each trace was averaged from two to fourteen responses. Intensities (photons $\mu\text{m}^{-2} \text{s}^{-1}$) from below upwards, were: 3.31×10^4 ; 1.03×10^5 ; 3.32×10^5 ; 1.04×10^6 . Bandwidth 0–20 Hz. *B*, normalized response amplitude (\bar{r}) as a function of step intensity at the four times after step onset indicated by the arrows in *A*. Normalizing constant was the maximal response amplitude of 12 pA. Smooth curves have the form of curve III in Fig. 2, the weighted average of an exponential saturation and a Michaelis relation. The curves indicate the expected amplitude of the step response at the peak and plateau derived from the measured response amplitude/stimulus strength relation for brief flashes. Cell 14 of Table 1.

evoked responses scaled linearly with flash strength. In this linear region, the responsiveness may be characterized by the flash sensitivity, S_F , defined as the peak amplitude of the flash response divided by flash strength. Collected results from experiments on four cones are presented in Fig. 8, which plots flash sensitivity, normalized to the original flash sensitivity in darkness, as a function of normalized

background light intensity. The continuous curve was drawn according to the Weber–Fechner relation:

$$S_F/S_F^D = \frac{1}{1 + I/I_0}, \quad (8)$$

in which S_F^D is the initial flash sensitivity in darkness, S_F is the flash sensitivity in the presence of a steady background light of intensity I , and I_0 is the intensity that

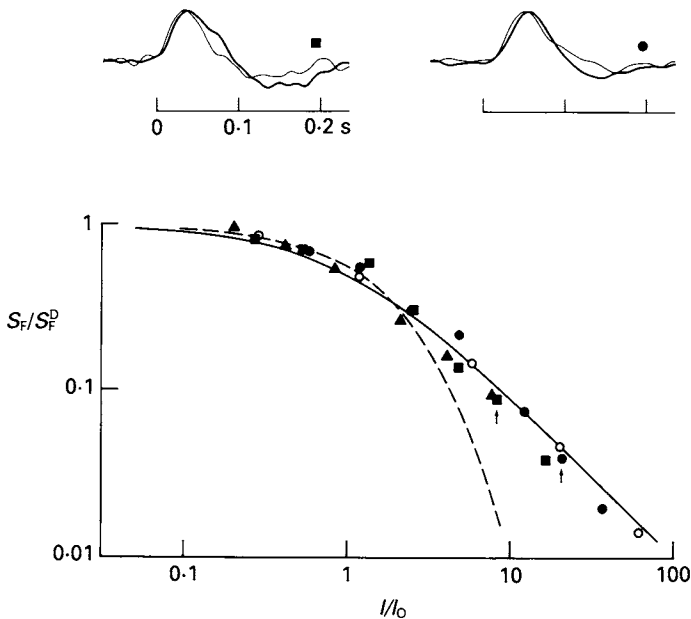


Fig. 8. Dependence of incremental flash sensitivity on background light intensity. Plot above collects results from four cones. Normalized flash sensitivity (sensitivity in presence of background divided by original sensitivity in darkness) shown as a function of normalized background intensity (intensity divided by intensity I_0 that gave a flash sensitivity of half the original dark sensitivity). The points are corrected for pigment bleaching as described in the text. Continuous curve drawn according to the Weber–Fechner relation, eqn (8) of text. Dashed curve shows the relation expected for one of the cells (\blacktriangle) if there were no time-dependent desensitization but instead a linear superposition of elementary excitations followed by an instantaneous saturation of the form of curve III in Fig. 2. Cell parameters I_0 (photons $\mu\text{m}^{-2} \text{s}^{-1}$), $i_{1/2}$ (photons μm^{-2}), r_{max} (pA), and τ_1 (ms) were: 2.5×10^4 , 1.33×10^3 , 12, 20 (\bullet); 2.0×10^4 , 7.00×10^3 , 10, 154 (\circ); 1.0×10^5 , 1.02×10^3 , 13, 8 (\blacktriangle); 1.4×10^5 , 2.5×10^3 , 15, 10 (\blacksquare). Filled and open symbols denote results from green- and red-sensitive cones respectively. Traces above show the form of dim flash responses in darkness (bold line) and in background light (thin line) from cells indicated by symbols; arrows in plot below indicate points derived from these incremental responses. Origin of time axes is centre of the incremental flash. Peak amplitudes of the incremental responses were 1–2 pA; responses have been scaled to the same arbitrary amplitude to allow comparison of the waveforms.

makes $S_F/S_F^D = 0.5$. This expression provides a reasonable description of the results. Values of I_0 ranged between 2.0×10^4 and 1.4×10^5 photons $\mu\text{m}^{-2} \text{s}^{-1}$. The mean value for I_0 was 7.1×10^4 photons $\mu\text{m}^{-2} \text{s}^{-1}$, corresponding to 3.3 log trolands.

In the experiments of Fig. 8 the bright background lights inevitably bleached

appreciable fractions of the pigment, and because the pigment epithelium was absent, no significant regeneration of pigment occurred. Bleaching will lower the effective intensity of a background light and the effective strength of an incremental flash. The points in Fig. 8 were corrected for these effects in the following way. A cone's mean relative pigment content during each background exposure was found from the cumulative applied photon density, assuming that the cone pigment in free solution had a photosensitivity of $8 \times 10^{-9} \mu\text{m}^2$ (see p. 699). The nominal background intensity and incremental flash strength were then multiplied by the mean relative pigment concentration during the exposure. The largest correction was for a relative concentration of 0.43. The desensitization illustrated in Fig. 8 cannot be attributed to a reduction in pigment density.

The dashed line in Fig. 8 shows the desensitization expected in one of the cells (\blacktriangle) if saturation alone caused the desensitization. This curve is the scaled derivative of the function used to fit the cell's instantaneous flash response saturation (curve III of Fig. 2). Consistent with the interpretation of Fig. 7, response saturation plays a role in desensitizing at low levels of background light, but in backgrounds above I_0 the time-dependent mechanism becomes significant and serves to protect the incremental response from saturation.

The traces at the top of Fig. 8 show normalized photocurrents evoked by brief flashes in darkness (bold lines) or in background light (thin lines). The background had only a small effect on the shape of the responses in spite of appreciable changes in incremental sensitivity. In some cells the responses speeded up slightly, but there was less than a 20% reduction in the time to peak for even the brightest backgrounds. The speeding was much less pronounced than that observed in turtle cones (Baylor & Hodgkin, 1974).

Figure 9 shows an attempt to determine the time course of background desensitization during a 1 s pulse of moderate intensity. Dim test flashes were used to probe the state of the cell before, during and after the conditioning pulse. Superimposed recordings from the experiment are shown above. The filled circles in the plot below give the normalized peak amplitude of the incremental flash response on the same time base as the current recording. These points were derived by subtracting the response to the pulse alone from the combined response to the flash and pulse and normalizing the amplitude with respect to that of the response to the flash alone.

To obtain the time course of the slow desensitization we assumed that the instantaneous saturation had the form of eqn (5), which fitted the intensity dependence of the cell's flash responses. Thus the measured photocurrent $j(t)$ is given by

$$j(t) = r_{\max}(1 - e^{-Y(t)}), \quad (9)$$

where $Y(t)$, termed the linearized response, is proportional to the elementary excitation and depends linearly on light intensity at short times. The open circles in Fig. 9 show the fall in the linearized incremental response that developed slowly in background light. These points were calculated by subtracting the linearized response to the pulse alone from the linearized response to the pulse and flash. The peak amplitude of this difference was plotted relative to that of the linearized response to the flash alone.

Although the resolution is limited, it appears that the time-dependent desensitization developed after a lag and was largely complete by about 0.5 s. The slow component accounted for little of the initial desensitization but a substantial fraction of that at the end of the pulse. The time-dependent desensitization had disappeared

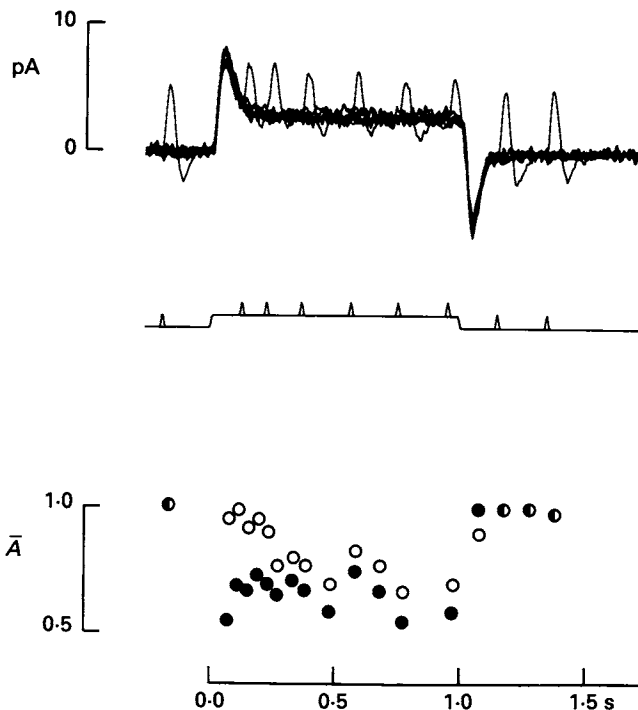


Fig. 9. Time course of desensitization during a pulse of light in a green-sensitive cone. Upper traces, superimposed recordings of outer segment current relative to dark level. Each trace shows the response to the conditioning pulse with a test flash superimposed, averaged from five to thirty-one sweeps. Stimulus monitor below records. Intensity of the conditioning pulse 8.00×10^4 photons $\mu\text{m}^{-2} \text{s}^{-1}$ and flash strength 1.72×10^3 photons μm^{-2} . Bandwidth 0–50 Hz. Maximal photocurrent 18 pA. The plot below shows the relative amplitude of the test response (\bar{A}) on the time scale of the upper traces. ●, amplitude of response to flash and pulse minus response to pulse alone, divided by amplitude of flash response in darkness. ○, relative amplitude of test response corrected for instantaneous non-linearity using eqn (9) of text. Cell 15 of Table 1.

about 0.2 s after the end of the conditioning pulse. These interpretations are consistent with those mentioned in connection with Fig. 7.

Figure 10 examines the changes in flash sensitivity that conditioning flashes produced in the cell of Fig. 9. The middle panel shows the responses to conditioning flashes of two different strengths. The upper panel shows the responses to incremental flashes applied at varying intervals, with the conditioning response subtracted. The filled circles in the lower panel plot the normalized peak amplitude of the incremental response; the open circles plot the normalized amplitude after correction for instantaneous saturation, using the procedure described above. The uncorrected amplitude increased during the undershoot in the conditioning response when more

channels were available to be blocked. The linearized amplitude fell and then rose to the original level because of the time-dependent desensitization.

Photosensitivity and the effects of bleaching on flash sensitivity

Exposing a cone to a light bright enough to bleach a substantial fraction of its pigment caused a proportional reduction in flash sensitivity but did not change the

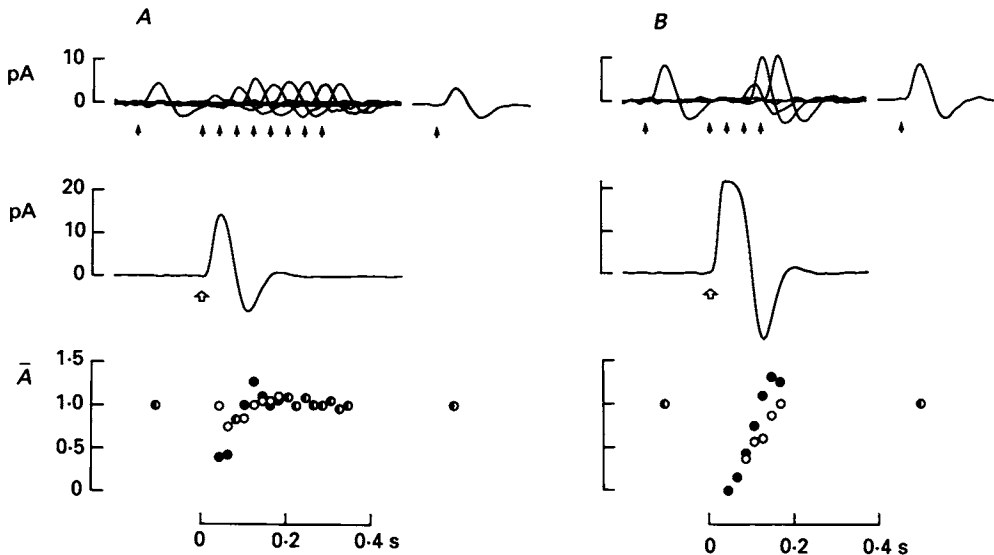


Fig. 10. Sensitivity changes after a conditioning flash in the green-sensitive cone of Fig. 9. In each panel the middle trace shows the response to the conditioning flash, which was delivered at the time indicated by the open arrow and had a strength of 2.25×10^8 photons μm^{-2} in *A* and 1.90×10^4 photons μm^{-2} in *B*. The upper traces show averaged responses to test flashes during the conditioning response, with the response to the conditioning flash removed by subtraction. Timing of the test flashes indicated by the filled arrows. Flash strengths were 5.31×10^2 photons μm^{-2} in *A*, and 1.77×10^3 photons μm^{-2} in *B*. Bandwidth 0–30 Hz. Maximal photocurrent 18 pA. The plot below shows the relative amplitude of the test response (\bar{A}) on the time scale of the upper traces. ●, amplitude of response to test flash and conditioning flash minus response to conditioning flash alone, divided by amplitude of test response in darkness. ○, relative amplitude of test response corrected for instantaneous non-linearity using eqn (9) of text. Cell 15 of Table 1.

response kinetics or saturating response amplitude. Results illustrating this point are presented in Fig. 11. Between each response family in Fig. 11*A* the red-sensitive cone was exposed to a 10 s light of fixed intensity at 2.55×10^7 photons $\mu\text{m}^{-2} \text{s}^{-1}$. The relations between peak response amplitude and flash strength are plotted in Fig. 11*B*. The continuous curves have the form of eqn (6). Each bleach decreased the normalized flash sensitivity k by a factor of 4.3 times, from 5.1×10^{-5} to 6.4×10^{-7} photons $^{-1} \mu\text{m}^2$.

The change in k can be explained in the following way. In the absence of the pigment epithelium, regeneration of bleached pigment should be minimal and therefore each bleaching exposure will lower the cone's pigment content and its flash

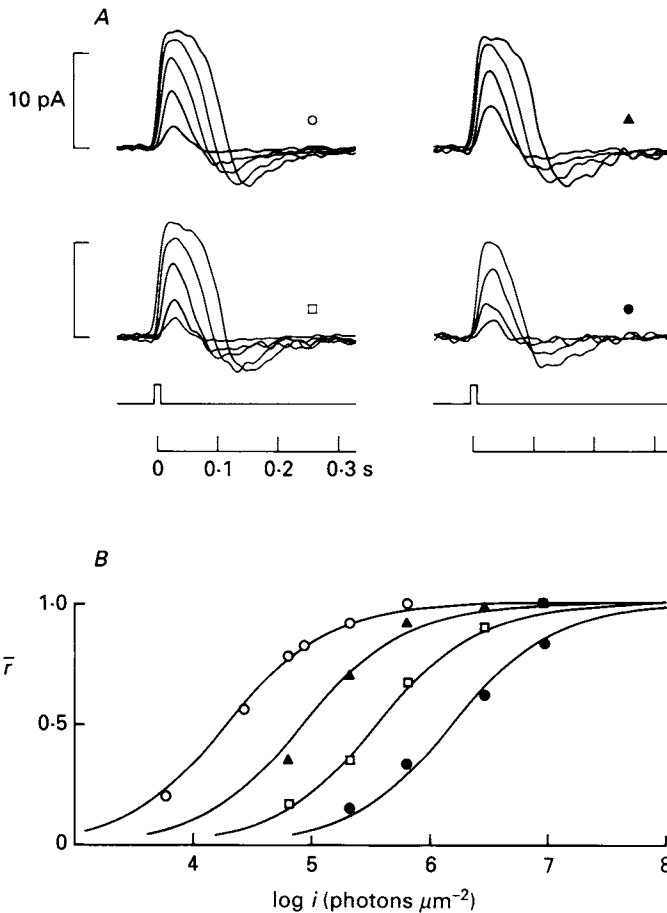


Fig. 11. Effect of bleaching on flash responses from a red-sensitive cone. *A*, response families to flashes of increasing strength; stimulus monitor below. Before each family was obtained the cone was exposed to a 10 s bleaching light of intensity 2.55×10^7 photons $\mu\text{m}^{-2} \text{s}^{-1}$. Each trace the average of two to thirteen sweeps. Digitally filtered, DC-25 Hz. *B*, normalized peak photocurrent amplitude \bar{r} , relative to the saturating amplitude of 12 pA, as a function of flash photon density; some responses illustrated in *A*. Smooth curves are Michaelis relations (eqn 6). For the curve at the left, k was taken as 5.13×10^{-6} photons $^{-1} \mu\text{m}^2$; each succeeding curve was drawn with k 4.3 times smaller, as expected if each bleaching exposure lowered the amount of pigment by this factor and if sensitivity varied inversely with pigment content. The photosensitivity P , obtained as described in the text, was $5.7 \times 10^{-9} \mu\text{m}^2$, corresponding to $7.6 \times 10^{-9} \mu\text{m}^2$ in free solution.

sensitivity by a fixed factor. After a bleaching exposure of intensity I and duration T the fraction f of unbleached pigment will be

$$f = \exp(-PTI). \quad (10)$$

The constant P in this expression is the photosensitivity (Dartnall, 1972), the product of the molecular cross-section for absorption and the quantum efficiency of photoisomerization. If a 4.3-fold reduction in flash sensitivity results from the same reduction in f , the known intensity and duration of the bleaching light can be used

in eqn (10) to calculate that the apparent value for P is $5.7 \times 10^{-9} \mu\text{m}^2$. This value will be only $\frac{3}{4}$ that in free solution because orientation of the pigment's dipole transition moment parallel to the sac membranes lowers the absorption of unpolarized light. The corresponding photosensitivity in free solution therefore would be $7.6 \times 10^{-9} \mu\text{m}^2$.

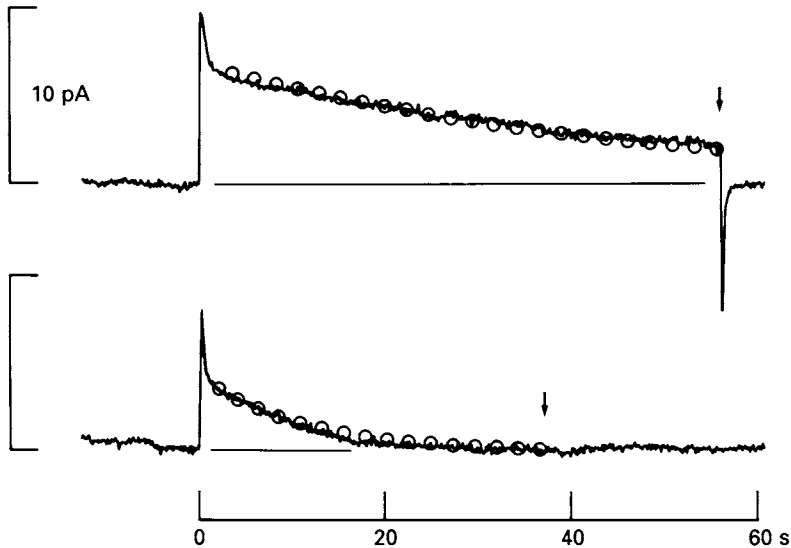


Fig. 12. Decline of a green-sensitive cone's photocurrent during bleaching pulses. Continuous traces plot membrane current as a function of time after onset of the bleaching pulse. Arrows above current traces indicate ends of bleaching pulses. Bleaching intensity was 1.02×10^7 photons $\mu\text{m}^{-2} \text{s}^{-1}$ for the upper trace and 4.24×10^7 photons $\mu\text{m}^{-2} \text{s}^{-1}$ for the lower. The circles plot exponential decays with time constants of 45 s (upper) and 11 s (lower); the time constants are inversely proportional to the light intensities. From the time constants and light intensities the apparent value of P was $2.2 \times 10^{-9} \mu\text{m}^2$ ($2.9 \times 10^{-9} \mu\text{m}^2$ in free solution). Saturating response 13 pA. Bandwidth 0.3 Hz. Cell 13 of Table 1.

This is comparable to that of rhodopsin in free solution, $1.0 \times 10^{-8} \mu\text{m}^2$ (Dartnall, 1972). The form and magnitude of the bleaching effects in Fig. 11 are thus consistent with a simple rule: bleaching changed the flash sensitivity by reducing the cone's ability to absorb. The cell in Fig. 11 exhibited similar behaviour over a still wider range of pigment content. A bleaching exposure was given prior to obtaining the first family in Fig. 11 and although an entire flash family was not recorded before this first bleach, the change in the linear responses indicated yet another four-fold sensitivity reduction. The interpretation therefore is that in this experiment the pigment content and flash sensitivity were proportional over a range of $(4.3)^4 = 342$ times. A similar experiment on a green-sensitive cone gave comparable results, with a photosensitivity (in free solution) of $8.7 \times 10^{-9} \mu\text{m}^2$.

The photosensitivity could also be estimated by fitting the decay of the photocurrent during a steady bleaching light, as illustrated in Fig. 12. The green-sensitive cone was exposed to bleaching lights at intensities of 1.0×10^7 photons $\mu\text{m}^{-2} \text{s}^{-1}$ (upper trace) and 4.2×10^7 photons $\mu\text{m}^{-2} \text{s}^{-1}$ (lower trace) for the times

indicated. Each response consisted of a spike when the light went on followed by a slowly declining outward current. The brighter light bleached nearly all of the cone's pigment, for there was no undershoot when the light was turned off, and no further responses could be obtained with the brightest light available (not illustrated).

The circles fitted to the decays are exponentials with time constants of 45 and 11 s, which are inversely proportional to the respective bleaching intensities. This behaviour is consistent with the idea that after the spike the photocurrent amplitude at any instant was proportional to the photoisomerization rate, which in turn was proportional to the fraction of unbleached pigment in the cone. Making this assumption, P may be calculated from $(I\tau_b)^{-1}$, where τ_b is the exponential decay constant. In this cell, $P = 2.2 \times 10^{-9} \mu\text{m}^2$, corresponding to a free solution value of $2.9 \times 10^{-9} \mu\text{m}^2$. As expected, exponential decays were observed only when the photocurrent had an amplitude less than about $\frac{1}{3}$ maximal, so that response saturation was minimal. In the cell of Fig. 12 the amplitudes of the exponential phases were small relative to the saturating amplitude of 13 pA because substantial pigment had previously been bleached.

Measurements similar to that in Fig. 12 were made on a total of five cells. For two red-sensitive cones P was (free solution values) 5.6×10^{-9} and $6.7 \times 10^{-9} \mu\text{m}^2$, while for three green-sensitive cones the values were 2.9×10^{-9} , 4.1×10^{-9} and $7.9 \times 10^{-9} \mu\text{m}^2$. The scatter in the figures suggests that this method, which is susceptible to baseline drift, is less accurate than the other. In the red-sensitive cone illustrated in Fig. 11 the photosensitivity was measured by both methods, and the photosensitivities were in reasonable agreement: $7.9 \times 10^{-9} \mu\text{m}^2$ (flash family method) and $5.6 \times 10^{-9} \mu\text{m}^2$ (photocurrent decline in steady light).

Values for P measured from the rate of decline of the photocurrent are likely to be lower limits, for response saturation and the time course of the cone response to light will slow the decay. Values measured by the method in Fig. 11 will be upper limits if bleached pigment itself desensitizes the transduction mechanism. The reasonable agreement between the photosensitivities determined in the two ways suggests that bleached pigment had little effect on the size or shape of the single-photon response. The situation is strikingly different in rods, where bleached pigment desensitizes transduction and produces a long-lasting residual excitation (e.g. Lamb, 1980; Schnapf, Kraft, Nunn & Baylor, 1987). The general conclusion is that the red- and green-sensitive cone pigments have a photosensitivity of about $8 \times 10^{-9} \mu\text{m}^2$, comparable to that of rhodopsin.

Analysis of light-induced noise

Although the single photon response of the cones is too small to be directly resolved, analysis of light-induced fluctuations in membrane current can give information about the quantal response. Figure 13A illustrates the increase in noise that occurred during a red-sensitive cone's response to steady dim light. If the noise is a superposition of quantal responses that have the shape of the dim flash response and occur in a Poisson stream, the power spectrum of the noise will have the form of the spectrum of the dim flash response. Figure 13B compares the difference spectrum of the cone's light-induced noise with the spectrum of its average dim flash response. The spectra had peaks at about 4 Hz and coincided at higher frequencies;

the noise spectrum was not well resolved at low frequency. Although this experiment might suggest a systematic difference between the low-frequency portions of the two spectra, such a difference was not a consistent observation in other experiments and we are inclined to think that it reflects poor resolution of the noise spectrum. In a total of five experiments of this type the spectrum of the light-induced noise had the general form of the difference spectrum in Fig. 13*B*, with a peak at 3.5–7 Hz. We conclude that the quantal event underlying the light-induced noise had a shape roughly like that of the dim flash response.

If the quantal responses have an invariant size and shape and are linearly additive, the peak amplitude a of the response may be obtained from

$$a = \sigma^2 s / \mu, \quad (11)$$

where σ^2 is the variance increase in light, μ the mean amplitude of the steady response, and s is the 'shape factor' characteristic of the quantal event (Katz & Miledi, 1972), given by

$$s = \frac{\int_{t=0}^{\infty} j(t) dt}{\int_{t=0}^{\infty} j^2(t) dt} = \frac{\tau_i}{\tau_s}. \quad (12)$$

Here $j(t)$ is the quantal response normalized to a peak amplitude of one, τ_i is the integration time or effective duration of the response, and τ_s is the effective duration of the squared response. In five cones, s was 0.44 ± 0.13 (mean \pm s.d.).

Analysis of the dim flash response of the red-sensitive cone of Fig. 13 gave a value for s of 0.34. The value of a , estimated by applying eqn (11) was 32 fA. The ratio $\mu/a\tau_i$ gives the mean frequency of occurrence of quantal responses, from which the effective collecting area A_c can be calculated from the applied light intensity. For the cone in Fig. 13, A_c was estimated in this way as $0.59 \mu\text{m}^2$.

Experiments of this type were performed on a total of five cones, three red-sensitive and two green-sensitive. The value of a was 17.7 ± 8.7 fA (mean \pm s.d.), while A_c was $0.44 \pm 0.27 \mu\text{m}^2$. The largest value for a was obtained from the cone of Fig. 13, which had a saturating response amplitude of 28 pA, and we shall assume that an a of about 30 fA is characteristic of the best cells. The estimate of a depends on the assumption that the quantal events have identical amplitudes. Variations in quantal amplitude would contribute to the measured variance and cause a to be overestimated (Katz & Miledi, 1972).

Dark noise

The filled circles in Fig. 14 show the power spectrum of the current recorded from a green-sensitive cone in darkness. The Johnson noise expected from the electrode leakage resistance had the density indicated by the dashed line. The small magnitude of this component suggests that most of the noise was generated by the cone itself. Tests in two other cells confirmed this notion; when the membrane current shut off briefly during a bright light the noise fell to near the calculated Johnson level. The dark spectrum in Fig. 14 contained a broad peak near 7 Hz and an additional lobe extending to higher frequencies. The open circles, which plot the spectrum in dim

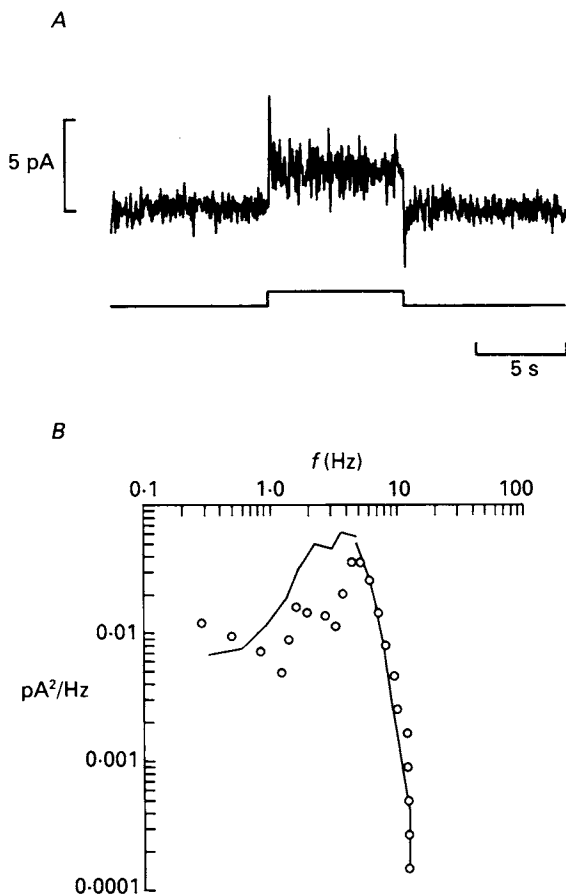


Fig. 13. Light-induced fluctuations in a red-sensitive cone's membrane current. *A*, dim light of intensity 3.78×10^3 photons $\mu\text{m}^{-2} \text{s}^{-1}$ was applied at the time indicated by the monitor trace. Bandwidth 0–10 Hz. *B*, power spectral density of light-induced noise (\circ) compared with spectrum of dim flash response (line). Noise spectrum is the difference between spectra in light and dark, calculated from twenty-two sweeps in the dark and five sweeps in the light. For frequencies up to 5 Hz, the spectrum was averaged over five frequency points before computing the difference; for frequencies above 5 Hz, averaging was over ten points. Spectrum of the dim flash response was computed from the average flash response shown in Fig. 3*B*. This spectrum was averaged over five frequency points at frequencies above 5 Hz and plotted without averaging below 5 Hz; the final spectrum was shifted vertically to give the best match to the points at high frequencies. Recording bandwidth 0–80 Hz for noise spectrum and 0–100 Hz for flash response spectrum. Cell 7 of Table 1.

light, show an elevation in noise at low frequency. The light-induced noise in Fig. 14 rolls off at two-fold higher frequency than that in Fig. 13. This difference parallels a roughly two-fold difference in the kinetics of the responses to dim flashes recorded from the two cells.

We suppose that the peak at 7 Hz in the dark spectrum may arise from spontaneously occurring events with a shape like that of the photon-induced response. Perhaps the lobe extending to high frequency arises from gating noise in

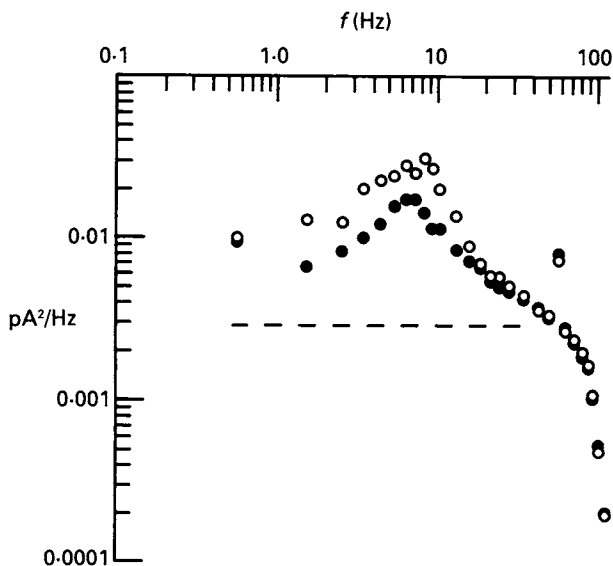


Fig. 14. Power spectral density of a green-sensitive cone's current noise in darkness (●) and in dim light (○) of intensity 1.54×10^4 photons $\mu\text{m}^{-2} \text{s}^{-1}$. Dashed line shows the Johnson noise level for the $5.9 \text{ M}\Omega$ electrode leakage resistance. Variance in the dark was 0.51 pA^2 , in the light 0.63 pA^2 , bandwidth 0–100 Hz. Spectra calculated from twenty-five sweeps in the dark, twenty-one in the light. For plotting, the spectra were averaged over five frequency points in the range 0–10 Hz, fifteen points (10–30 Hz), or forty points (30–100 Hz). Cell 18 of Table 1.

the light-sensitive channels (Bodoia & Detwiler, 1985). The lower frequency portion of the noise, within the band 0–20 Hz, is important physiologically because it will limit detection of very dim light. The variance of this component, corrected by subtraction of the Johnson variance, was determined from experiments on five cells as $0.125 \pm 0.045 \text{ pA}^2$ (mean \pm s.d.). In each experiment the spectrum of the dark noise had a form similar to that in Fig. 14, with a peak near 5–7 Hz. The low frequency dark variance may be expressed as a 'dark light', I_D^* , the photoisomerization rate that would generate noise with the same variance. From Campbell's theorem (Katz & Miledi, 1972):

$$I_D^* = \sigma_D^2 A_c / a^2 \tau_s, \quad (13)$$

where σ_D^2 is the dark variance corrected for the Johnson noise (0–20 Hz). Taking a as 20 fA and τ_s as 49 ms (the average in five cells) gives I_D^* as $2.4 \times 10^3 \text{ s}^{-1}$, or 170 trolands. This is nearly identical to Lamb & Simon's (1977) value of $2.8 \times 10^3 \text{ s}^{-1}$ for turtle cones. We were surprised to find that bleaching a cone's pigment (99% or more) reduced the low-frequency peaked component of the dark noise even though the dark current recovered. In each of three cones, bleaching reduced the variance; the average reduction in the corrected variance (0–20 Hz) was 20%. The molecular mechanism of this reduction remains to be determined.

DISCUSSION

Photosensitivity

The red- and green-sensitive cone pigments had photosensitivities near $8 \times 10^{-9} \mu\text{m}^2$ (free solution values) in the two best experiments. This is of the same order as estimates from work of other investigators. By analysing the early receptor potential of cones in turtle eyecups, Hodgkin & O'Bryan (1977) found an apparent photosensitivity of $8 \times 10^{-9} \mu\text{m}^2$. Although their free solution value is difficult to ascertain because of uncertainty about the incident angle of the light, it would lie between 5.3×10^{-9} and $1.6 \times 10^{-8} \mu\text{m}^2$. Densitometric measurements on cone pigments in the intact human eye gave photosensitivities of $1.4 \times 10^{-8} \mu\text{m}^2$ (Rushton & Henry, 1968) and $1.6 \times 10^{-8} \mu\text{m}^2$ (Geisler, 1981), using the trolands conversion indicated in Methods, and recalculating to the free solution values. Although further photosensitivity measurements on the cone pigments are needed, comparison of the values available with that of rhodopsin ($1.0 \times 10^{-8} \mu\text{m}^2$, Dartnall, 1972), shows that cone pigments bleach with an efficiency comparable to that of rhodopsin.

Intensity dependence of cone signals

The flash sensitivity of monkey cones is similar to that of turtle cones and higher than that of squirrel cones when expressed as the peak fractional reduction in the light-sensitive conductance that results from a single photoisomerization. For monkey cones the figure was about 1/1000, compared to an estimate of 1/630 for turtle cones (Baylor & Hodgkin, 1973) and about 1/10000 for squirrel cones (Kraft, 1988).

Presumed cone responses in electroretinographic recordings from the macaque retina (Boynton & Whitten, 1970; Valetton & van Norren, 1983) were reported to vary with light intensity I according to $I^n/(I^n + I_{\frac{1}{2}}^n)$, where the constant $n = 0.74$ and the half-saturating intensity $I_{\frac{1}{2}}$ was 3.3–4.2 log trolands (corrected for the different retinal magnification factors of the macaque and human eye). Similar intensities were needed here to elicit a half-saturating step response (3.0 and 3.3 log trolands for the peak and plateau respectively). The sublinear dependence on the intensity of dim stimuli was not observed here. In this study as well as in earlier measurements on single cones (Baylor & Hodgkin, 1973; Kraft, 1988), responses to dim stimuli obeyed strict criteria for linearity.

In psychophysical experiments it is difficult to saturate the cone system with a prolonged bright light, but incremental sensitivity can be transiently saturated by brief background exposures at intensities exceeding 4 log trolands (Hood, Ilves, Maurer, Wandell & Buckingham, 1978; Geisler, 1978). The measured flash sensitivity of single cones was greatly reduced by response saturation at similar intensities, and it seems attractive to suppose that the psychophysical effect reflects closure of the cone's light-sensitive channels. In a similar way, it was concluded that scotopic saturation was a consequence of channel saturation in rod outer segments (Baylor *et al.* 1984).

During the undershoot in the response to a conditioning flash the sensitivity to a second flash increased as more channels became available to close. A corresponding

reduction in visual thresholds has been detected psychophysically when a background pulse is extinguished (Geisler, 1978).

Kinetics of linear responses

Strongly diphasic flash responses have not been observed in recordings from cones of other animals. For example, a turtle cone's response to a dim flash is monophasic when the flash is presented in darkness and becomes only slightly diphasic in the presence of background light (e.g. Baylor & Hodgkin, 1974). Nevertheless the kinetics that we have observed seem consistent with other results on the negative feedback loop in the outer segment if the light-induced pulse of PDE activity is short compared to the impulse response of the loop itself. Indeed, when the PDE pulse was assumed to outlast the photocurrent (Hodgkin & Nunn, 1988) the more familiar monophasic responses were calculated from eqn (19). Direct measurements of the turnover times of cyclic GMP and free calcium would be useful tests of the kinetic model. Interestingly, the dark noise in some turtle cones had a resonant spectrum, even though the dim flash responses were monophasic (Lamb & Simon, 1977). This seems consistent with the idea that the noise is due to brief pulsatile fluctuations within a similar feedback loop, and that the light-elicited PDE pulse in turtle cones is relatively more prolonged.

Do the cones in the intact primate retina give diphasic responses? Focal recordings of massed responses from the macaque retina have been interpreted to indicate that the step response lacks an initial transient (Valeton & van Norren, 1982, 1983). Nevertheless, Whitten & Brown (1973, e.g. Fig. 3) obtained foveal responses very similar to those in Fig. 3*B* here. Baron & Boynton (1975) as well as Valeton & van Norren (1982) recorded aspartate-isolated cone responses with 'on' and 'off' transients. Furthermore, the 5–10 Hz peak in the flicker sensitivity of human cone vision is consistent with a diphasic cone impulse response (Watson, 1986). The amplitude spectrum of the dim flash response shown in Fig. 14 has the same general form as the flicker sensitivity of human cone vision. This correspondence is expected if central neurons receive cone signals with kinetics like those observed here.

A possible objection is that the shape of the psychophysical flicker sensitivity function depends strongly on experimental conditions. In particular, when the flicker is delivered on a pattern containing high spatial frequencies or when the retina is thoroughly dark adapted, the resonant peak of the flicker function disappears, leaving a function characteristic of a low-pass filter. These effects might be explained by assuming that central neurons that are dark adapted or that have small receptive fields low-pass filter the cone signals more severely, thus truncating the peak in the flicker curve. An alternative explanation is that cone signals positive to the resting membrane potential are not readily transferred to higher-order neurons. This might occur if, in the dark, postsynaptic channels were nearly saturated by the cone neurotransmitter. The saturation would be relieved by applying background lights that hyperpolarized the cone and reduced the rate of transmitter release. The saturation would be exacerbated by stimuli of small retinal area, as larger signals would be required of fewer cones, causing more truncation of the undershoot.

Geisler (1981) has proposed that a diphasic cone response might account for the 'subtractive adaptation' inferred from psychophysical measurements. This process

is assumed to attenuate responses to a steady light while leaving responses to light increments undisturbed.

Comparison of cone types

Psychophysical measurements of flicker sensitivity at different wavelengths (Brindley, Du Croz & Rushton, 1966) suggested that the blue-sensitive cone system is slower than the red and green systems. Although we studied only three blue-sensitive cones in detail, their kinetics and sensitivities were similar to those of the red- and green-sensitive cones. It seems likely that the sluggishness of the blue system reflects properties of central neurons rather than properties of the cones themselves. The finding that the green-sensitive cone step response was more transient than that of red-sensitive cones is consistent with Green's (1969) flicker sensitivity measurements, which showed that the green mechanism had a more pronounced fall-off at low temporal frequency.

Light adaptation

The adaptation of monkey cones in background light differed quantitatively from that of turtle cones in several respects. A background causing about 3×10^4 photoisomerizations s^{-1} halved the flash sensitivity of monkey cones, whereas in turtle cones the corresponding rate was an order of magnitude lower (Baylor & Hodgkin, 1974). This difference is partly attributable to the lower integration time of the monkey cones, but the monkey cones also required a larger steady fractional reduction in dark current to produce a given reduction in incremental sensitivity. Furthermore, background light shortened the time scale of the dim flash response dramatically in turtle cones (Baylor & Hodgkin, 1974) but had little effect on the kinetics of the incremental response in the monkey cones. These differences may be summarized by the statement that monkey cones behaved linearly to higher light levels.

A light-induced drop in intracellular Ca^{2+} mediates background adaptation in salamander rods and cones (Matthews, Murphy, Fain & Lamb, 1988; Nakatani & Yau, 1988). If the feedback loop in Fig. 15 produces the undershoot in the flash response of monkey cones, what is responsible for the desensitization (Fig. 7) that develops on a much slower time scale? Perhaps both the undershoot and desensitization are triggered by a fall in the level of intracellular Ca^{2+} , with the fall occurring in two phases. In addition to the fast drop responsible for the undershoot there might be a slower drop that parallels the fall in intracellular Na^+ resulting from channel closure and persistent operation of the Na^+-K^+ pump. By increasing $Na^+/Ca^{2+}-K^+$ exchange a lowered internal Na^+ would lower intracellular Ca^{2+} . In an outer segment with the dimensions observed here, a dark current of 30 pA, and an internal Na^+ concentration of 10 mM, the internal Na^+ should change on a time scale comparable to that of the slow desensitization. An alternative explanation is that a high-affinity intracellular buffer for Ca^{2+} might slow the final decline.

Psychophysical studies have shown that background light desensitizes cone vision at levels that had little effect on transduction in the cones as measured in the present experiments. The threshold for cone vision is doubled by a 1–2 log troland background (Hood & Finkelstein, 1986), whereas intensities of roughly 3.3 log trolands were required to halve the flash sensitivity of a single cone. A similar

discrepancy was found between scotopic incremental sensitivity and the sensitivity of single rods (Baylor *et al.* 1984). The implication is that visual thresholds are not fixed by the size of the quantal responses in the outer segments.

Dark noise

Primate cones were noisier than primate rods in darkness, the variances of the currents being about 0.12 and 0.023 pA² respectively in the band 0–20 Hz (Baylor *et al.* 1984). Similarly, the dark rate of cyclic GMP turnover, as estimated from fitting the flash response (Fig. 6), was about 20 times higher than that estimated for amphibian rods (Hodgkin & Nunn, 1988). Both these observations are consistent with a pulsatile spontaneous activation of PDE, which occurs at a higher mean rate in cones than in rods.

Psychophysical experiments indicate that a 1 min of arc diameter test flash of 550 nm light can be detected reliably when it delivers at least 600 photons to the cornea (Hood & Finkelstein, 1986). A flash of this intensity would elicit roughly 32 photoisomerizations per cone (see Methods). Given the size of the quantal responses and the magnitude of the dark noise measured here, could the cone's response to such a stimulus be resolved? The photopic system appears to integrate information over a single cone and over a period of roughly 50 ms (Hood & Finkelstein, 1986). For an equivalent dark rate of 2400 photoisomerizations cone⁻¹ s⁻¹, an average of 120 equivalent photoisomerizations are expected within this 50 ms period, with a standard deviation of 11 photoisomerizations. Thus, the signal elicited by the weakest resolvable test flash would exceed the standard deviation of the noise by a factor of three.

Psychophysical estimates of cone dark light fall in the range of about 1–50 trolands (e.g. Barlow, 1958; Geisler, 1978). These values are lower than the equivalent intensity of about 170 trolands estimated here from current fluctuations in single cones. This discrepancy remains unexplained.

APPENDIX

The purpose of this section is to present a mathematical treatment of the light responses expected from the feedback mechanism discussed on p. 690. A similar analysis of the system has been presented by Hodgkin (1988), who derived the response to a step change in the rate of operation of the Na⁺/Ca²⁺-K⁺ exchanger. Here we derive the response to a light-induced increase in phosphodiesterase activity.

In analysing the time-dependent behaviour of this feedback system we make two important simplifications. (a) All concentrations are taken to be uniform within the region affected by absorption of a photon, the effects of spatial gradients being ignored. This may be a reasonable approximation for excitation in a cone sac which is isolated by narrow connections to other sacs but within which diffusional equilibrium is achieved rapidly. (b) The effects of cyclic GMP on the membrane and the effect of Ca²⁺ on the guanylate cyclase are linearized. While non-linear interactions as well as diffusional gradients are likely to have some influence on the kinetics of the photocurrent, this simplified treatment may help to interpret the gross features of the oscillatory flash response.

Under the conditions outlined above, the feedback system of Fig. 15 is described by the following equations:

$$\frac{dG}{dt} = \alpha - \beta G, \quad (14a)$$

$$\frac{dC}{dt} = \gamma - \delta C, \quad (14b)$$

$$\alpha = \alpha_0(1 + b\Delta C/C_0), \quad (14c)$$

$$\gamma = \gamma_0(1 + c\Delta G/G_0), \quad (14d)$$

where

G = concentration of cyclic GMP,

C = concentration of free Ca^{2+} ,

α = rate of cyclic GMP synthesis by guanylate cyclase (GC),

β = rate constant of cyclic GMP hydrolysis by phosphodiesterase (PDE),

γ = rate of Ca^{2+} influx,

δ = rate constant of Ca^{2+} exchange,

$G_0, C_0, \alpha_0, \beta_0, \gamma_0,$ and δ_0 are the dark steady-state values of the above quantities,

Δ denotes the deviation of these values from the dark level,

b = sensitivity of α to changes in C , i.e. $b = (\Delta\alpha/\alpha_0)/(\Delta C/C_0)$, and

c = sensitivity of γ to changes in G , i.e. $c = (\Delta\gamma/\gamma_0)/(\Delta G/G_0)$.

Excitation by light leads to a change in β . Since eqns (14a-d) are linear, the system is completely described by its impulse response. Let x and y denote the relative changes in G and C , i.e. $x(t) = \Delta G(t)/G_0$ and $y(t) = \Delta C(t)/C_0$. Then eqns (14) become

$$\frac{dx(t)}{dt} = \beta_0[by(t) - x(t)] - \Delta\beta(t),$$

and

$$\frac{dy(t)}{dt} = \delta_0[cx(t) - y(t)].$$

By standard methods one finds that the response, $x_1(t)$, to an impulse change in β is given by

$$x_1(t) = e^{-pt} \left[\frac{g}{q} \sinh(qt) - \cosh(qt) \right], \quad (15)$$

where

$$p = \frac{1}{2}(1/\tau_{cG} + 1/\tau_{Ca}),$$

$$g = \frac{1}{2}(1/\tau_{cG} - 1/\tau_{Ca}),$$

$$q = (g^2 + bc/\tau_{cG}\tau_{Ca})^{0.5},$$

$$\tau_{cG} = 1/\beta_0,$$

and

$$\tau_{Ca} = 1/\delta_0.$$

Here, τ_{cG} and τ_{Ca} are the dark turnover times for cyclic GMP and Ca^{2+} respectively. The response to an arbitrary time course of PDE activity, $\Delta\beta(t)$, is given by

$$x(t) = \int_{t'=-\infty}^t \Delta\beta(t') x_1(t-t') dt', \quad (16)$$

and the current, $J(t)$, through the outer segment membrane becomes

$$J(t) = J_0[1 + cx(t)], \tag{17}$$

where J_0 denotes the dark value of the membrane current.

In the model, the properties of the feedback loop are determined entirely by the dark turnover times τ_{cG} and τ_{Ca} and the overall loop gain, bc . If the gain is large and

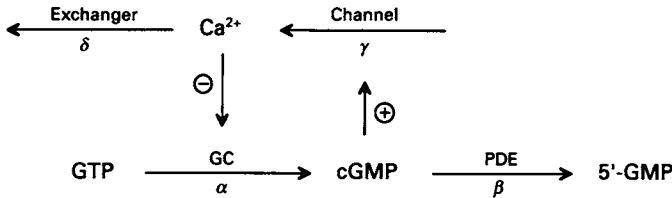


Fig. 15. Diagram of feedback model for cone transduction. The channel-controlling substance 3'-5'-cyclic guanosine monophosphate (cGMP) is synthesized by the guanylate cyclase (GC) at rate α and hydrolysed by the phosphodiesterase (PDE) with a rate constant β . Calcium ions (Ca^{2+}) enter through open channels at rate γ and are removed from the cell by $Na^+/Ca^{2+}-K^+$ exchange, which operates with rate constant δ . Cyclic GMP opens membrane channels, increasing γ , while Ca^{2+} inhibits the guanylate cyclase, reducing α . Thus the two intracellular messengers are connected in a closed, negative gain feedback loop which stabilizes the dark state. A flash of light perturbs the system by transiently increasing β . This model is based on work in many laboratories (reviewed in Hodgkin, 1988 and Stryer, 1988).

negative, that is $bc < -g^2 \tau_{cG} \tau_{Ca}$, then q is imaginary, and the impulse response becomes oscillatory:

$$x_1(t) = e^{-pt} \left[\frac{g}{\omega} \sin(\omega t) - \cos(\omega t) \right],$$

where the frequency of oscillation $\omega = (-g^2 - bc/\tau_{cG} \tau_{Ca})^{0.5}$.

The time course of the light-induced rise in PDE activity is not known. The simplest assumption, that the flash causes an instantaneous rise followed by an exponential decay, gave a good fit to most of the flash response but did not reproduce the S-shaped initial delay. The entire waveform was fitted by assuming that the pulse of PDE activity took the form of the output of three sequential low-pass filters with identical time constants, τ_{PDE} :

$$\Delta\beta(t) = B(t/\tau_{PDE})^2 \exp(-t/\tau_{PDE}), \tag{18}$$

where B is a scalar. From eqns (16) and (17), the photocurrent expected from the driving function given in eqn (18) is:

$$j(t) = \Delta J(t) = J_0 cB \left\{ \left(\frac{g}{q} - 1 \right) u_{\downarrow}(t) - \left(\frac{g}{q} + 1 \right) u_{\uparrow}(t) \right\}, \tag{19}$$

where

$$u_{\pm}(t) = \frac{\tau_{PDE}}{[1 - \tau_{PDE}(p \pm q)]^3} \left\{ e^{-(p \pm q)t} - e^{-t/\tau_{PDE}} \sum_{m=0}^2 \frac{[t(1/\tau_{PDE} - (p \pm q))]^m}{m!} \right\},$$

and p , g and q are defined as in eqn (15). The theoretical curves for the photocurrent in Fig. 6A were calculated from eqn (19). We assumed gain factors of $c = 3$ (Zimmerman & Baylor, 1986) and $b = -4$ (Koch & Stryer, 1988). The values of τ_{CG} , τ_{Ca} , τ_{PDE} and B were adjusted to provide the best fit to the measured responses.

This work was supported by grants from Research to Prevent Blindness, Inc., the Helen Hay Whitney Foundation, the Lucille P. Markey Charitable Trust, and grants EY05750 and EY07642 from the National Eye Institute, USPHS. We thank Mr Robert Schneeveis for technical assistance.

REFERENCES

- BARLOW, H. B. (1958). Intrinsic noise of cones. In *Visual Problems of Colour*, vol. 2, pp. 617–630. HM Stationery Office, London.
- BARON, W. S. & BOYNTON, R. M. (1975). Response of primate cones to sinusoidally flickering homochromatic stimuli. *Journal of Physiology* **246**, 311–331.
- BAYLOR, D. A. & HODGKIN, A. L. (1973). Detection and resolution of visual stimuli by turtle photoreceptors. *Journal of Physiology* **234**, 163–198.
- BAYLOR, D. A. & HODGKIN, A. L. (1974). Changes in time scale and sensitivity in turtle photoreceptors. *Journal of Physiology* **242**, 729–758.
- BAYLOR, D. A., HODGKIN, A. L. & LAMB, T. D. (1974). The electrical response of turtle cones to flashes and steps of light. *Journal of Physiology* **242**, 685–727.
- BAYLOR, D. A., LAMB, T. D. & YAU, K.-W. (1979). Responses of retinal rods to single photons. *Journal of Physiology* **288**, 613–634.
- BAYLOR, D. A., NUNN, B. J. & SCHNAPF, J. L. (1984). The photocurrent, noise and spectral sensitivity of rods of the monkey *Macaca fascicularis*. *Journal of Physiology* **357**, 575–607.
- BAYLOR, D. A., NUNN, B. J. & SCHNAPF, J. L. (1987). Spectral sensitivity of cones of the monkey *Macaca fascicularis*. *Journal of Physiology* **390**, 145–160.
- BODOIA, R. D. & DETWILER, P. B. (1985). Patch-clamp recordings of the light-sensitive dark noise in retinal rods from the lizard and frog. *Journal of Physiology* **367**, 183–216.
- BOYNTON, R. M. & WHITTEN, D. N. (1970). Visual adaptation of monkey cones: recordings of late receptor potentials. *Science* **170**, 1423–1426.
- BRINDLEY, G. S., DU CROZ, J. J. & RUSHTON, W. A. H. (1966). The flicker fusion frequency of the blue-sensitive mechanism of colour vision. *Journal of Physiology* **183**, 497–500.
- CERVETTO, L., LAGNADO, L., PERRY, R. J., ROBINSON, D. W. & McNAUGHTON, P. A. (1989). Extrusion of calcium from rod outer segments is driven by both sodium and potassium gradients. *Nature* **337**, 740–743.
- COLQUHOUN, D. & SIGWORTH, F. L. (1983). Fitting and statistical analysis of single-channel records. In *Single-Channel Recording*, ed. SAKMANN, B. & NEHER, E., pp. 191–264. Plenum, New York.
- DARTNALL, H. J. A. (1972). Photosensitivity. In *Handbook of Sensory Physiology*, vol. VII/1, *Photochemistry of Vision*, ed. DARTNALL, H. J. A., pp. 122–145. Springer-Verlag, New York.
- GEISLER, W. S. (1978). Adaptation, afterimages and cone saturation. *Vision Research* **18**, 279–289.
- GEISLER, W. S. (1981). Effects of bleaching and backgrounds on the flash response of the cone system. *Journal of Physiology* **312**, 413–434.
- GREEN, D. G. (1969). Sinusoidal flicker characteristics of the color-sensitive mechanisms of the eye. *Vision Research* **9**, 591–601.
- HAROSI, F. I. (1975). Absorption spectra and linear dichroism of some amphibian photoreceptors. *Journal of General Physiology* **66**, 357–382.
- HODGKIN, A. L. (1988). Modulation of ionic currents in vertebrate photoreceptors. *Proceedings of the Retina Research Foundation Symposium* **1**, 6–30.
- HODGKIN, A. L. & NUNN, B. J. (1988). Control of light-sensitive current in salamander rods. *Journal of Physiology* **403**, 439–471.
- HODGKIN, A. L. & O'BRYAN, P. M. (1977). Internal recording of the early receptor potential in turtle cones. *Journal of Physiology* **267**, 737–766.

- HOOD, D. C. & FINKELSTEIN, M. A. (1986). Sensitivity to light. In *Handbook of Perception and Human Performance*, vol. 1, *Sensory Processes and Perception*, ed. BOFF, K. R., KAUFMAN, L. & THOMAS, J. P., pp. 5/1-5/66. Wiley, New York.
- HOOD, D. C., ILVES, T., MAURER, E., WANDELL, B. & BUCKINGHAM, E. (1978). Human cone saturation as a function of ambient intensity: a test of models of shifts in the dynamic range. *Vision Research* **18**, 983-993.
- KATZ, B. & MILEDI, R. (1972). The statistical nature of the acetylcholine potential and its molecular components. *Journal of Physiology* **224**, 665-699.
- KOCH, K.-W. & STRYER, L. (1988). Highly cooperative control of retinal rod guanylate cyclase by calcium ions. *Nature* **334**, 64-66.
- KRAFT, T. W. (1988). Photocurrents of cone photoreceptors of the golden-mantled ground squirrel. *Journal of Physiology* **404**, 199-213.
- LAMB, T. D. (1980). Spontaneous quantal events induced in toad rods by pigment bleaching. *Nature* **287**, 349-351.
- LAMB, T. D., McNAUGHTON, P. A. & YAU, K.-W. (1981). Spatial spread of activation and background desensitization in toad rod outer segments. *Journal of Physiology* **319**, 463-496.
- LAMB, T. D. & SIMON, E. J. (1977). Analysis of electrical noise in turtle cones. *Journal of Physiology* **272**, 435-468.
- MATTHEWS, H. R., MURPHY, R. L. W., FAIN, G. L. & LAMB, T. D. (1988). Photoreceptor light adaptation is mediated by cytoplasmic calcium concentration. *Nature* **334**, 67-69.
- NAKATANI, K. & YAU, K.-W. (1988). Calcium and light adaptation in retinal rods and cones. *Nature* **334**, 69-71.
- PICCOLINO, M. & GERSCHENFELD, H. M. (1978). Activation of a regenerative calcium conductance in turtle cones by peripheral stimulation. *Proceedings of the Royal Society B* **201**, 309-315.
- RUSHTON, W. A. H. & HENRY, G. H. (1968). Bleaching and regeneration of cone pigments in man. *Vision Research* **8**, 617-631.
- SCHNAPF, J. L., KRAFT, T. W. & BAYLOR, D. A. (1987). Spectral sensitivity of human cones. *Nature* **325**, 439-441.
- SCHNAPF, J. L., KRAFT, T. W., NUNN, B. J. & BAYLOR, D. A. (1987). Spectral sensitivity and dark adaptation in primate photoreceptors. *Investigative Ophthalmology and Visual Science* **28/3**, 50.
- SCHNAPF, J. L. & MCBURNEY, R. N. (1980). Light-induced changes in membrane current of cone outer segments of tiger salamander and turtle. *Nature* **287**, 239-241.
- STRYER, L. (1988). Molecular basis of visual excitation. *Cold Spring Harbor Symposia on Quantitative Biology* **53**, 283-294.
- VALETON, J. M. & VAN NORREN, D. (1982). Fractional recording and component analysis of primate LERG: separation of photoreceptor and other retinal potentials. *Vision Research* **22**, 381-391.
- VALETON, J. M. & VAN NORREN, D. (1983). Light-adaptation of primate cones: an analysis based on extracellular data. *Vision Research* **23**, 1539-1547.
- WATSON, A. B. (1986). Temporal sensitivity. In *Handbook of Perception and Human Performance*, vol. 1, *Sensory Processes and Perception*, ed. BOFF, K. R., KAUFMAN, L. & THOMAS, J. P., pp. 6/1-6/43. Wiley, New York.
- WHITTEN, D. N. & BROWN, K. T. (1973). The time courses of late receptor potentials from monkey cones and rods. *Vision Research* **13**, 107-135.
- WYSZECKI, G. & STILES, W. S. (1982). *Color Science. Concepts and Methods, Quantitative Data and Formulae*. Wiley, New York.
- ZIMMERMAN, A. L. & BAYLOR, D. A. (1986). Cyclic GMP-sensitive conductance of retinal rods consists of aqueous pores. *Nature* **321**, 70-72.